In honour of Nicola Cabibbo, father of flavour physics.
He introduced the idea of universality between the leptonic current and a single hadronic current, combination of the $SU(3)$ currents allowing $\Delta S = 0$ and $\Delta S = 1$ transitions. It was thus Nicola Cabibbo who reconciled strange particle decays with the the universality of weak interactions paving the way to the modern electroweak unification within the Standard Model.

New UT*fit* Analysis of the Unitarity Triangle in the Cabibbo-Kobayashi-Maskawa scheme

Marcella Bona,[1] Marco Ciuchini,[2] Denis Derkach,[3] Fabio Ferrari,[4,5] Enrico Franco,[6] Vittorio Lubicz,[2,7] Guido Martinelli,[6,8] Davide Morgante,[9,10] Maurizio Pierini,[11] Luca Silvestrini,[6] Silvano Simula,[2] Achille Stocchi,[12] Cecilia Tarantino,[2,7] Vincenzo Vagnoni,[4] Mauro Valli,[13] and Ludovico Vittorio[14]

(The **UT***fit* Collaboration)

[1] *School of Physics and Astronomy, Queen Mary University of London, London; United Kingdom*
[2] *INFN, Sezione di Roma Tre, Via della Vasca Navale 84, I-00146 Rome, Italy*
[3] *HSE University, 20 Myasnitskaya Ulitsa, Moscow 101000, Russia*
[4] *INFN, Sezione di Bologna, Via Irnerio 46, I-40126 Bologna, Italy*
[5] *Dipartimento di Fisica e Astronomia, Università di Bologna, Viale Berti Pichat 6/2, 40127 Bologna, Italy*
[6] *INFN, Sezione di Roma, P.le A. Moro 2, I-00185 Roma, Italy*
[7] *Dipartimento di Matematica e Fisica, Università Roma Tre, Via della Vasca Navale 84, I-00146 Rome, Italy*
[8] *Dipartimento di Fisica, Università di Roma La Sapienza, P.le A. Moro 2, I-00185 Roma, Italy*
[9] *INFN, Sezione di Milano, Via Celoria 16, I-20133 Milano, Italy*
[10] *Dipartimento di Fisica, Università degli Studi di Milano, Via Celoria 16, I-20133 Milano, Italy*
[11] *CERN CH-1211 Geneve 23, Switzerland*
[12] *Université Paris Saclay, CNRS/IN2P3, IJCLab, 91405 Orsay, France*
[13] *C.N. Yang Institute for Theoretical Physics, Stony Brook University, Stony Brook, NY 11794, USA*
[14] *LAPTh, Université Savoie Mont-Blanc and CNRS, Annecy, France*

Flavour mixing and CP violation as measured in weak decays and mixing of neutral mesons are a fundamental tool to test the Standard Model (SM) and to search for new physics. New analyses performed at the LHC experiment open an unprecedented insight into the Cabibbo-Kobayashi-Maskawa (CKM) metrology and new evidence for rare decays. Important progress has also been achieved in theoretical calculations of several hadronic quantities with a remarkable reduction of the uncertainties. This improvement is essential since previous studies of the Unitarity Triangle did show that possible contributions from new physics, if any, must be tiny and could easily be hidden by theoretical and experimental errors. Thanks to the experimental and theoretical advances, the CKM picture provides very precise SM predictions through global analyses. We present here the results of the latest global SM analysis performed by the UTfit collaboration including all the most updated inputs from experiments, lattice QCD and phenomenological calculations.

I. INTRODUCTION

In this paper we enlarge and update the Unitarity Triangle Analysis within the Standard Model (SM) using the most recent progress of the theoretical inputs and the latest measurements of the experimental observables. A more general analysis beyond the SM, with constraints on new physics contributions, will be presented in a subsequent publication.

The **UT***fit* collaboration has been routinely updating the Unitarity Triangle Analysis (UTA) within and beyond the SM via its online results (http://utfit.org/), regular presentations to topical conferences and continuous collaboration with the flavour community, see [1–4] and references therein. Within the SM, the UTA is a fundamental tool to determine precisely the SM parameters of the flavour sector, to test the compatibility of the experimental results with the theoretical calculations and to predict yet unmeasured flavour SM observables. Beyond the SM a quantitative evaluation of the degree of discrepancy between measurements and theoretical predictions offers the possibility of discovering New Physics (NP) effects due to the presence of new particles or interactions at still unexplored energy scales. In this respect, the UTA is complementary to the search of new particles at colliders working at multi-TeV energies. For a recent discussion about predictions of rare decays in the SM see [5].

Within the SM, flavour mixing and weak CP violation are described by several free parameters, namely the quark masses and the CKM matrix elements [6, 7]. Indeed these parameters can be reduced to only ten independent, physically determinable quantities, that we choose to be the quark masses, m_q, defined in a suitable scheme, and the

value of the Wolfenstein parameters $\lambda, \mathcal{A}, \bar{\rho}, \bar{\eta}$ [8, 9]. In addition, the SM is characterised by two important properties: the absence of tree-level Flavour Changing Neutral Currents (FCNC) and the GIM suppression mechanism [10]. The latter manifests itself either as *mild GIM* suppression, proportional to $\log m_q^2/M_W^2$, for QCD and radiative penguin operators/amplitudes, or as *hard GIM* suppression, proportional to m_q^2/M_W^2, for $\Delta F = 2$ transitions. Thus, beyond the SM, CKM and/or GIM suppressed processes are the most interesting quantities to study since they are highly sensitive to NP contributions. Among them, $\Delta F = 2$ transitions are the best cases since they are both CKM and *hard GIM* suppressed. This is the reason why accurate SM estimates of CP violation in neutral meson oscillations is a crucial ingredient of the UTA analysis that we will discuss in the following.

In the recent past, there has been a lot of excitement about apparent violations of Lepton Flavour Universality (LFU). On the one hand, in the case of semileptonic decays, we have the so-called $|V_{cb}|$ puzzle, i.e. the tension between the inclusive [11–13] and the exclusive determinations of the CKM matrix element $|V_{cb}|$ [14–21]. On the other hand, a discrepancy exists between the theoretical expectation value and the measurements of $R(D^{(*)})$ [22], defined as the ratios of the branching fractions of $B \to D^{(*)}\tau\nu_\tau$ over $B \to D^{(*)}\ell\nu_\ell$ decays, $\ell = e, \mu$, performed by Belle, BaBar and LHCb [23–31]. For $|V_{cb}|$ we included in our analysis the latest experimental measurements and the results of a new approach to evaluate the form factors based on unitarity and analyticity. Besides semileptonic charged-current B decays, LFU seems to be violated by the ratios $R_{K^{(*)}} = BR(B \to K^{(*)}\mu^+\mu^-)/BR(B \to K^{(*)}e^+e^-)$ which are sensibly lower than the value close to one expected if LFU holds [32–35]. Although the UTA is not able to shed any light on the $R_{K^{(*)}}$ (and $R(D^{(*)})$) problem, it is very useful to clarify the issues connected to the $|V_{cb}|$ puzzle, since a determination of this CKM matrix element can be derived indirectly from the UTA when omitting the exclusive and inclusive semileptonic B decays in the inputs. In addition to the new values for $|V_{cb}|$ from exclusive decays, our updated analysis is also based on the latest determinations of other relevant theoretical inputs and recent measurements of the experimental flavour observables. The basic constraints used in the global fit and contributing to the sensitivity of the CKM matrix elements are: $|V_{ub}|$ and $|V_{cb}|$ from semileptonic B decays, ΔM_d and ΔM_s from $B^0_{d,s}$ oscillations, ε from neutral K^0 mixing, the unitarity triangle angles α from charmless hadronic B decays, γ from charm hadronic B decays and $\sin 2\beta$ from $B^0 \to J/\psi K^0$ decays. To these *classical* quantities, we added $\mathrm{BR}(B^+ \to \tau^+\nu_\tau)$, $\mathrm{BR}(B_s \to \mu^+\mu^-)$ and the ratio ε'/ε for which a solid theoretical prediction now exists [36]. Although the present precision is not enough to further constrain the parameters of the SM, we believe that is important to include this quantity in view of further theoretical improvements and also because it can help to constrain the contribution of some operators present in models of NP. In the present work we also included a new evaluation of long distance charm contributions to ε [37].

The values of most experimental inputs are taken from the Heavy Flavour Averaging Group (HFLAV) [22] and from the online update. When updated individual results are available, however, the UTfit collaboration performs its own averages. We also use the updates of the Particle Data Group 2022 [38]. On the theoretical side, the non-perturbative QCD parameters are taken from the most recent Lattice QCD (LQCD) determinations: as a general prescription, we average the $N_f = 2+1+1$ and $N_f = 2+1$ FLAG numbers [39]. The continuously updated set of numerical values used as inputs can be found at the URL http://www.utfit.org/.

As for the output results of the UTA and their uncertainties, for all fits the quoted numbers correspond to the highest probability intervals containing at least 68% and 95% of the sample. The 68% probability intervals are then presented as $V(E_V)$, where V is the center and E_V the half width of the interval.

The main results of this work are the following: i) there is a general consistency, at the percent level, between the SM predictions and the experimental measurements. Thus in order to discover new physics effects a further effort in theoretical and experimental accuracy is required; ii) although the tension between exclusive and inclusive determination of $|V_{cb}|$ requires further investigation, in particular of the form factors relevant in semi-leptonic $B \to D^{(*)}\ell\nu_\ell$ decays and of the fitting procedures of these processes, we find that the UT analysis strongly favours a larger value of $|V_{cb}|$, close to its inclusive determination, and a smaller value of $|V_{ub}|$, close to the exclusive value; iii) the value of ε'/ε as predicted by using the weak Hamiltonian operator matrix elements computed in ref. [36] and the Wilson coefficients computed within the general UT analysis are in very good agreement with the experimental value whereas the **UT***fit* prediction for ε is lower than its experimental value and a further improvement in the accuracy of the theoretical calculation is welcome. The results of this work, written for the *Rendiconti Lincei. Scienze Fisiche e Naturali*, will be combined with an **UT***fit* analysis of D^0-$\bar{D}^0$ mixing and of searches for physics beyond the Standard Model in a paper to be submitted to a physics journal.

The paper is organized as follows: in sec. II we describe the theoretical and experimental inputs used in our analysis; in sec. III we discuss the recent progress in the calculation of the CP violating amplitudes related to ε and ε'/ε, which is included in our analysis for the first time; in sec. IV we present the results of our updated analysis in the Standard Model. Finally, in sec. V we present our conclusion and an outlook for future developments.

Input	Reference	Measurement	**UT***fit* Prediction	Pull
$\sin 2\beta$	[22], **UT***fit*	0.688(20)	0.736(28)	-1.4
γ	[22]	66.1(3.5)	64.9(1.4)	$+0.29$
α	**UT***fit*	94.9(4.7)	92.2(1.6)	$+0.6$
$\varepsilon \cdot 10^3$	[38]	2.228(1)	2.00(15)	$+1.56$
$\lvert V_{ud}\rvert$	**UT***fit*	0.97433(19)	0.9738(11)	$+0.03$
$\lvert V_{ub}\rvert \cdot 10^3$ •	**UT***fit*	3.77(24)	3.70(11)	$+0.25$
$\lvert V_{ub}\rvert \cdot 10^3$ (excl)	[39]	3.74(17)		
$\lvert V_{ub}\rvert \cdot 10^3$ (incl)	[22]	4.32(29)		
$\lvert V_{cb}\rvert \cdot 10^3$ •	**UT***fit*	41.25(95)	42.22(51)	-0.59
$\lvert V_{cb}\rvert \cdot 10^3$ (excl)	**UT***fit*	39.44(63)		
$\lvert V_{cb}\rvert \cdot 10^3$ (incl)	[40]	42.16(50)		
$\lvert V_{ub}\rvert/\lvert V_{cb}\rvert$	[39]	0.0844(56)		
$\Delta M_d \times 10^{12}\,\mathrm{s}^{-1}$	[38]	0.5065(19)	0.519(23)	-0.49
$\Delta M_s \times 10^{12}\,\mathrm{s}^{-1}$	[38]	17.741(20)	17.94(69)	-0.30
$\mathrm{BR}(B_s \to \mu\mu) \times 10^9$	[38]	3.41(29)	3.47(14)	-0.14
$\mathrm{BR}(B \to \tau\nu) \times 10^4$	[38]	1.06(19)	0.869(47)	$+0.96$
$\mathrm{Re}\,(\varepsilon'/\varepsilon) \times 10^4$	[38]	16.6(3.3)	15.2(4.7)	$+0.27$
ϕ_ε	[38]	0.7596 rad		
ω	[38]	0.04454(12)		
$\delta_0(s)$ *	[38]	$32.3(2.1)^\circ$	$32.3(1.7)^\circ$ at $s = 471.0$ MeV [41]	
$\delta_2(s)$ *	[38]	$-11.6(2.8)^\circ$	$-7.96(37)^\circ$ at $s = 479.1$ MeV [41]	
$\mathrm{Re}\,(A_2)$	[38]**	$1.479(4) \times 10^{-8}$ GeV	$1.50(10) \times 10^{-8}$ GeV	
$\mathrm{Re}\,(A_0)$	[38]***	$3.3201(18) \times 10^{-7}$ GeV	$3.01(41) \times 10^{-7}$ GeV	
$\mathrm{Im}\,(A_0)$	**UT***fit*		$-6.75(86) \times 10^{-11}$ GeV	
$\mathrm{Im}\,(A_2)$	**UT***fit*		$-8.4(1.2) \times 10^{-13}$ GeV	

TABLE I. *Full SM inputs with their predictions from the SM global fit. When the averages are made by us, using values and errors from other calculations, the reference is denoted by* **UT***fit* *and the procedure used to obtain the final value and uncertainty is explained in the text.* • *These values have been obtained by combining the exclusive and inclusive values of* $|V_{ub}|$, $|V_{cb}|$ *and* $|V_{ub}|/|V_{cb}|$ *reported in this table as explained in sec. II A.* * *s denotes the c.o.m. energy of the two pions;* ** $\mathrm{Re}\,(A_2)$ *is extracted from the* $K^+ \to \pi^+\pi^0$ *decay widths;* *** $\mathrm{Re}\,(A_0)$ *is computed using the* $K^0 \to \pi^+\pi^-$ *and* $K^0 \to \pi^0\pi^0$ *decay widths as explained in the text. The theoretical values of* $\delta_{0,2}(s)$ *in the fourth column of the table have been taken from ref. [41].*

Input	Reference	Measurement
$\tau_{D^0} \cdot 10^{13} s$	[38]	0.4101 ± 0.0015
$\tau_{B^0} \cdot 10^{12} s$	[22]	1.519(4)
$\tau_{B^+} \cdot 10^{12} s$	[22]	1.638(4)
$\tau_{B_s} \cdot 10^{12} s$	[22]	1.516(6)
$\Delta\Gamma_s/\Gamma_s$	[22]	0.112(10)
$\alpha_s(M_Z)$	[42]	0.11792(94)
$m_t^{\overline{\mathrm{MS}}}(m_t^{\overline{\mathrm{MS}}})$ (GeV)	[42]	163.44(43)

TABLE II. *Extra inputs used in our UTA analysis. The quoted value of* $m_t^{\overline{\mathrm{MS}}}(m_t^{\overline{\mathrm{MS}}})$ *corresponds to* $m_t^{\mathrm{pole}} = (171.79 \pm 0.38)$ *GeV [40].*

II. UPDATE OF THEORETICAL AND EXPERIMENTAL INPUTS

In this section we discuss the main experimental and theoretical updated inputs that have been used in our UTA analysis. A list of the experimental inputs can be found in tables I and II. Most of the experimental inputs, as the values of the CKM matrix elements $|V_{ij}|$, are extracted from data using some theoretical calculation, e.g. the form factors in the case of semi-leptonic decays. We will also present a discussion of the decay constants, form factors and B-parameters used in this work with a comparison of the values used by other groups. Most of the inputs for these

Input	Lattice
$\hat{B}_K$	0.756(16)
f_{B_s}	230.1(1.2) MeV
f_{B_s}/f_B	1.208(5)
$\hat{B}_{B_s}$	1.284(59)
$\hat{B}_{B_s}/\hat{B}_B$	1.015(21)
$m_{ud}^{\overline{\rm MS}}(2\,{\rm GeV})$	3.394(29) MeV
$m_s^{\overline{\rm MS}}(2\,{\rm GeV})$	93.11(52) MeV
$m_c^{\overline{\rm MS}}(3\,{\rm GeV})$	991(5) MeV
$m_c^{\overline{\rm MS}}(m_c^{\overline{\rm MS}})$	1290(7) MeV
$m_b^{\overline{\rm MS}}(m_b^{\overline{\rm MS}})$	4196(14) MeV

TABLE III. *Full lattice inputs. The values of the different quantities have been obtained by taking the weighted average of the $N_f = 2+1$ and $N_f = 2+1+1$ FLAG numbers [39].*

non-perturbative QCD parameters are taken from the most recent lattice determinations and given in table III. As already mentioned, our general prescription is to take the weighted average of the $N_f = 2+1$ and $N_f = 2+1+1$ FLAG numbers [39]. We will discuss in this paper only those cases where we followed a different procedure and explain the reasons for the different choice.

In table I, the values denoted as **UT***fit* prediction in the fourth column are obtained from the UT analysis by excluding the quantity under consideration. Thus, for example, $|V_{cb}| \cdot 10^3 = 42.22(51)$ and $|V_{ub}| \cdot 10^3 = 3.70(11)$ have been obtained by excluding from the UT analysis the input values of these CKM matrix elements.

A. The CKM matrix elements

In this subsection we discuss the updated absolute values of several elements of the Cabibbo-Kobayashi-Maskawa (CKM) matrix [6, 7].

1. $|V_{ud}|$ and $|V_{us}|$

$|V_{ud}|$ and $|V_{us}|$ are determined from super allowed $0^+ \to 0^+$ nuclear β decays and from a combined analysis of $K_{\mu 2}$, $K_{\ell 3}$ and $\pi_{\mu 2}$ decays.

One possibility is the extraction of $|V_{ud}|$ and $|V_{us}|$ from the lattice determination of $f^+(0)$ and f_K/f_π using the relations [38, 43]

$$|V_{us}| f^+(0) = 0.2165(4)\,, \qquad \frac{|V_{us}| f_K}{|V_{ud}| f_\pi} = 0.2760(4)\,. \tag{1}$$

The lattice results for $f^+(0)$ or f_K/f_π have been obtained averaging the results of lattice calculations performed either within the four flavour, $N_f = 2+1+1$, or within the three flavour, $N_f = 2+1$, theory [39], the corresponding results for $|V_{ud}|$ and $|V_{us}|$ are given in table IV. The weighted average for $|V_{ud}|$ is

$$|V_{ud}| = 0.974387(98)\,. \tag{2}$$

In the past the super allowed nuclear β transitions provided the most precise determination of $|V_{ud}|$. Its accuracy is limited by the hadronic uncertainties of the electroweak radiative corrections, some of which are universal for all the nuclei whereas others depend on the specific nucleus structure. A new critical survey which takes into account the most recent experimental results and the new theoretical calculations of the radiative corrections [44–47] has been presented in ref. [48]. The average of the data, including radiative and isospin-symmetry-breaking corrections, yields the CKM matrix element

$$|V_{ud}| = 0.97373(31)\,, \tag{3}$$

the uncertainty of which is larger than the value quoted in Eq. (2). The value in Eq. (3) is lower than the previous 2015 result by one standard deviation and its uncertainty is increased by 50%. The variation is a consequence of new

	Reference	$\lvert V_{ud}\rvert$	$\lvert V_{us}\rvert$
β decay	[48]	0.97373 (31)	
$N_f = 2+1$	[39]	0.97438 (12)	0.2249 (5)
$N_f = 2+1+1$	[39]	0.97440 (17)	0.2248 (7)
τ decay	[22]	0.97561 (40)	0.2195 (19)
τ decay	[52, 53]	0.97461 (43)	0.2240 (18)

TABLE IV. *Values of $|V_{ud}|$ and $|V_{us}|$ from different physical processes. For completenesss we also give the values obtained from τ decays although they are not used in the present paper.*

calculations for the radiative corrections and of the spread between different estimates of these corrections. Hopefully, at least for the universal corrections, a new more accurate determination will come from lattice calculations. Indeed, only the easiest cases, namely the radiative corrections to $K_{\mu 2}$ and $\pi_{\mu 2}$ decays, have been computed so far on the lattice from first principles and without any model assumption/approximation [49, 50].

By combining with the PDG method [38] (see also ref. [51]) the most precise results from refs. [39] and [48], eqs. (2) and (3), we quote the final results

$$|V_{ud}| = 0.97433(19)\,, \qquad |V_{us}| = 0.2251(8)\,, \tag{4}$$

where $|V_{us}|$ is indeed obtained from the unitarity of the CKM matrix in the SM and it is therefore not used in the UTA. For a recent reappraisal of the determination of $|V_{ud}|$ and $|V_{us}|$ and of the problem of the unitarity of the first CKM matrix row see also ref. [54].

2. $|V_{cb}|$

Semileptonic $B \to D^{(*)}\ell\nu_\ell$ decays and their inclusive counter part are very important processes in the phenomenology of flavor physics. From their measurement and the corresponding theoretical predictions depends the value of $|V_{cb}|$ which plays a fundamental role in the UTA analyses [2, 55, 56]. For years we had to live with the apparent strong tension between the inclusive [11–13] and the exclusive determination of this CKM matrix element [14–21]. Some important novelties have, however, recently changed the previous situation: on the one hand the inclusive predictions were recently reconsidered and the uncertainties of the calculation performed in the Heavy Quark Effective Theory were reevaluated [40, 57]. On the other hand, new lattice calculations of the relevant form factors in the small recoil region [58], new approaches to their determination in the full kinematical range [59–63] and measurements of the exclusive differential decay rates were presented. We think that it is possible to argue that for $|V_{cb}|$, although some difference remains, the tension is finally resolved, see the recent average from ref. [62] given in eq. (9) below. A set of values from different estimates of $|V_{cb}|$ from inclusive and exclusive decays are given in table V.

For the exclusive determination of $|V_{cb}|$ we proceed as follows:

- For $B \to D^*$ semileptonic decays, rather than making an average of the values of $|V_{cb}|$ given in the rows 8-9 of table V, following the procedure adopted for other quantities in this paper, we average the form factor $F(1)$ obtained from $N_f = 2+1$, $F(1) = 0.906(13)$, and $N_f = 2+1+1$, $F(1) = 0.895(10)(24)$ [39], obtaining $F(1) = 0.904(11)$;
- Then, using the formula derived from the rate, $F(1)\,\eta_{EW}\,|V_{cb}| = 35.44(64)10^{-3}$ [39], and $\eta_{EW} = 1.00662$ [66] we get $|V_{cb}| = 38.95(86)10^{-3}$;
- For $B \to D$, following [39], we quote $|V_{cb}| = 40.0(1.0)10^{-3}$;
- Averaging the above values of $|V_{cb}|$ from $B \to D^*$ and $B \to D$ we obtain

$$|V_{cb}| \cdot 10^3 \ \ \text{(excl.)} = 39.44(65)\,. \tag{5}$$

This procedure uses all the available information from $B \to D^*$ but neglects the correlation of the lattice determination of form factors for $B \to D^*$ and $B \to D$ decays obtained using the same gauge field configurations. Alternatively, we combined the $N_f = 2+1$ value of $|V_{cb}|$ by FLAG, obtained by averaging $B \to D^*$ and $B \to D$ decays and taking into account the correlation of the lattice determination of form factors for these decays obtained using the same

	Process	Reference	$\lvert V_{cb}\rvert \cdot 10^3$
1	$b \to c$ inclusive	[40]	42.16 (50)
2	$B \to D$	[61] DM	41.0 (1.2)
3	$B \to D$ $N_f = 2+1$	[39]	40.0 (1.0)
4	$B_s \to D_s$ $N_f = 2+1$	[62] DM	41.7 (1.9)
5	$B \to D^*$	[63] DM	41.3 (1.7)
6	$B \to D^*$	[64]	39.6 (1.1)
7	$B \to D^*$	[65]	39.6 (1.1)
8	$B \to D^*$ $N_f = 2+1$	[39]	38.9 (0.9)
9	$B \to D^*$ $N_f = 2+1+1$	[39]	39.3 (1.4)[a]
10	$B \to D^*$ and $B \to D$ $N_f = 2+1$	[39]	39.4 (0.7)
11	$B_s \to D_s^*$ $N_f = 2+1$	[62] DM	40.7 (2.4)

TABLE V. *Values of $|V_{cb}|$ from inclusive or exclusive determinations. [a] This value of $|V_{cb}| \times 10^3$ has been derived using the value of the form factor at zero recoil given in Eq. (267) of ref.[39]. DM in the rows 2-4-5-11 denotes the values obtained by using the Dispersive Matrix approach mentioned in the text. For completenesss we also give some determinations which are not used in the present paper. More recent determinations of $|V_{cb}|$ from $B \to D^{(*)}$ semileptonic decays by Belle II have been presented at the 2022 ICHEP Conference in Bologna by T. Koga (KEK). Since, however, LQCD form factors and experimental data were simultaneously used to extract the value of $|V_{cb}|$, we decided not to use these results for the time being.*

gauge field configurations, $|V_{cb}| = 39.48(68)10^{-3}$, with the value that we can obtain from the form factor $F(1)$ with $N_f = 2+1+1$, $|V_{cb}| = 39.34(1.35)10^{-3}$. We obtain

$$|V_{cb}| \cdot 10^3 \ \ (\text{excl.}) = 39.45(61)\,, \tag{6}$$

from which, after combining using the PDG method [38] with the result in eq. (5), we get our final result

$$|V_{cb}| \cdot 10^3 \ \ (\text{excl.}) = 39.44(63)\,, \tag{7}$$

which differs by 3.4 σ from the inclusive value in table V. We may combine the inclusive value of $|V_{cb}|$ in table V with the result in Eq. (7) obtaining

$$|V_{cb}| \cdot 10^3 \ \ = 41.1(1.3) \ \ (\text{incl.} + \text{excl.})\,. \tag{8}$$

We anticipate that a more accurate determination of $|V_{cb}|$, that is the one used in this **UT***fit* analysis and quoted in Table I, will be obtained by combining Eq. (8) with the determination of $|V_{ub}|$ and of the ratio $|V_{ub}|/|V_{cb}|$ from $B_s \to (K^-, D_s^-)\mu^+\nu_\mu$ decays in Eq. (13).

An alternative determination of the exclusive value of $|V_{cb}|$ can be obtained by using the values obtained using the Dispersive Matrix (DM) approach of Ref. [59] and given in Table V, Refs. [61–63]. By combining these results, which include $B_s \to D_s^{(*)}$ decays, we obtain

$$|V_{cb}| \cdot 10^3 \ \ (\text{DM excl.}) = 41.2(8)\,, \tag{9}$$

namely a value much closer and compatible at the 1 σ level with the inclusive one, with an uncertainty comparable to the uncertainty quoted in Eq. (7) . By combining the inclusive value of Table V with the DM result in Eq. (9) we obtain the result

$$|V_{cb}| \cdot 10^3 \ \ = 41.9(4)(\text{incl.} + \text{DM excl.})\,, \tag{10}$$

more precise than the result of Eq. (8).

3. $|V_{ub}|$

The matrix element V_{ub} is determined from the measurements of the branching ratios of leptonic $B \to \tau\nu_\tau$ decays and from *exclusive* and *inclusive* semileptonic $b \to u$ decays. Theoretically, its precision is limited by the uncertainty of the calculations of the B meson decay constant and of the relevant form factors, for leptonic and exclusive semileptonic decays, and of the matrix elements of the operators appearing in the HQET expansion of the inclusive rate. For

$B \to \tau\nu_\tau$, which is very interesting because it is particularly sensitive to physics beyond the SM, the main source of uncertainty comes for the large error in the experimental measurement of the rate. Although the determinations from inclusive semileptonic decays are systematically higher than the exclusive ones, the two values are compatible, once the spread of the inclusive determinations using different theoretical models is considered.

For the leptonic decays we average the results given in Eqs. (289) and (290) of ref. [39] obtaining the value *a*) of eq. (11). For the exclusive semileptonic decays we take the number of table 57 of the same reference, quoted in *b*). We did not use the recent value of $|V_{ub}|$ from the Belle II Collaboration [67] since it is rather preliminary and based only on the form factors of the FNAL/MILC Collaboration [68]. We plan to include it in the future by using in the determination of $|V_{ub}|$, besides the form factors computed by FNAL/MILC, also the recently computed form factors by RBC/UKQCD [69] and JLQCD [70]. Finally, for inclusive semi-leptonic decays we use the value from ref. [22]. For completeness, we give the average of *a*) and *b*) in *d*); the average of *c*) and *d*) in *e*) and the average of *b*) and *c*) in *f*). We note that, in the case of the value of $|V_{ub}|$, a difference between the inclusive and exclusive determinations at the 1.7 σ level still persists, although with large relative errors.

We observe that the effect of including $B \to \tau\nu_\tau$ is almost invisible and, for reasons explained below, adopt in the following the average in *f*).

$$\begin{aligned}
V_{ub}^{B\to\tau} &= 4.05(64)\cdot 10^{-3} \quad a)\\
V_{ub}^{B\to\pi} &= 3.74(17)\cdot 10^{-3} \quad b)\\
V_{ub}^{\rm incl.} &= 4.32(29)\cdot 10^{-3} \quad c)\\
V_{ub}^{a+b} &= 3.76(16)\cdot 10^{-3} \quad d)\\
V_{ub}^{c+d} &= 3.89(24)\cdot 10^{-3} \quad e)\\
V_{ub}^{b+c} &= 3.89(25)\cdot 10^{-3} \quad f)
\end{aligned} \tag{11}$$

A percent precision is expected to be reached by LQCD using Exaflops CPUs for f_B and for the form factors entering the exclusive determination of $|V_{ub}|$. A higher precision will require the non-perturbative calculation of the radiative corrections to the decay rates [50]. Considering how challenging the measurement of $BR(B \to \tau\nu)$ in a hadronic environment is, it is difficult to imagine a similar improvement in precision of the experimental measurement for this channel for which a higher theoretical accuracy can be reached. On the other hand, it was pointed out in ref. [71] that the indirect determination of $|V_{ub}|$ from the fit in the SM is presently more accurate than the measurements, yielding a central value close to the *exclusive* determination. Therefore the most precise prediction of $BR(B \to \tau\nu)$ in the SM can be obtained by combining the *indirect* knowledge of $|V_{ub}|$ from the rest of the UT fit, fourth column in table I, combined with f_B derived from f_{B_s} and f_B/f_{B_s} in table III

$$BR(B \to \tau\nu)_{\rm UTfit} = 0.882(45)\,. \tag{12}$$

The progress of lattice calculations allow us to use in the analysis also the constraint coming from the ratio $|V_{ub}|/|V_{cb}|$ determined either from $\Lambda_b \to (p, \Lambda_c)\mu^-\bar\nu_\mu$ or $B_s \to (K^-, D_s^-)\mu^+\nu_\mu$ decays. We use only the latter decays since the lattice form factors relevant for Λ_b decays do not satisfy the quality criteria of FLAG [39]. Following [39] we quote

$$\frac{|V_{ub}|}{|V_{cb}|} = 0.0844(56)\,. \tag{13}$$

We have combined the information from exclusive and inclusive decays, eqs. (7) and (11)-b) and table V and eq. (11)-c) respectively, and the ratio $|V_{ub}|/|V_{cb}|$ in eq. (13) using the average procedure of refs. [51] obtaining the following input values that we have used in the present UT analysis

$$|V_{cb}|\cdot 10^3 = 41.25(95) \qquad |V_{ub}|\cdot 10^3 = 3.77(24)\,, \qquad \rho_c = 0.11 \tag{14}$$

where ρ_c is the correlation matrix element; had we used the results from the DM analysis, eq. (9), we would have obtained

$$|V_{cb}|\cdot 10^3 = 41.94(80) \qquad |V_{ub}|\cdot 10^3 = 3.79(24)\,, \qquad \rho_c = 0.09\,. \tag{15}$$

Had we used the most recent PDG value of $|V_{ub}|$ from inclusive decays [38], $|V_{ub}|\cdot 10^3 = 4.13(26)$, we would have obtained $|V_{cb}|\cdot 10^3 = 41.24(95)$ and $|V_{ub}|\cdot 10^3 = 3.76(23)$ with $\rho_c = 0.11$, substantially identical to the values given in Eq. (14), or, in the DM case, $|V_{cb}|\cdot 10^3 = 41.94(80)$ and $|V_{ub}|\cdot 10^3 = 3.77(23)$ with $\rho_c = 0.09$, substantially identical to the numbers of Eq. (15).

The values of the CKM matrix elements $|V_{ub}|$ and $|V_{cb}|$ from exclusive and inclusive decays, eqs. (7) and (11) and table V and eq. (11) respectively, and the ratio $|V_{ub}|/|V_{cb}|$ in eq. (13) are shown in the left plot of fig. 1. This figure

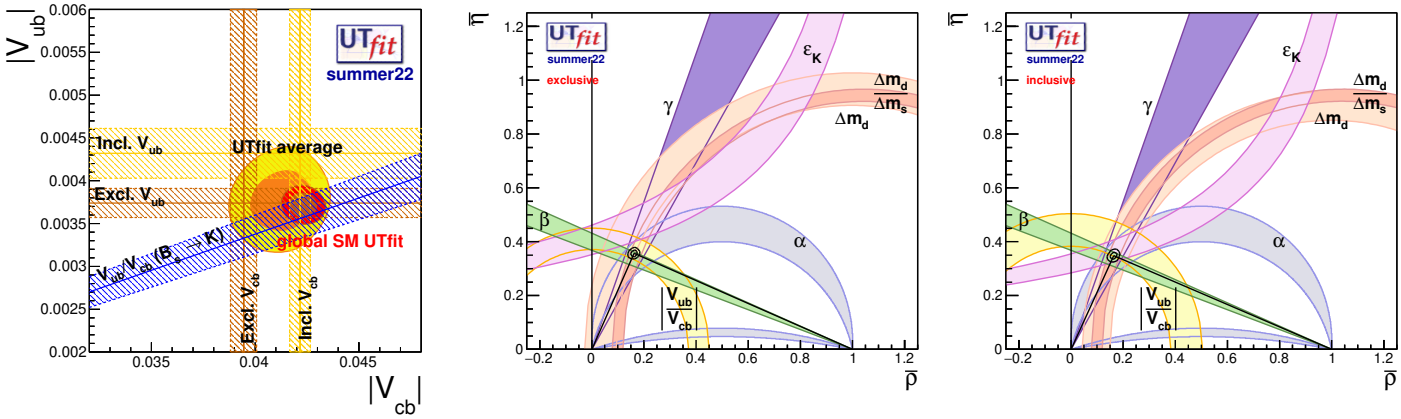

FIG. 1. *Left Panel: $|V_{cb}|$ vs $|V_{ub}|$ plane showing the values reported in Table I. We include in the figure the ratio $|V_{cb}|/|V_{ub}|$ from ref. [39] shown as a diagonal (blue) band; Central Panel: $\bar{\rho}$-$\bar{\eta}$ plane with the SM global fit results using only exclusive inputs for both V_{ub} and V_{cb}; Right Panel: SM global fit results using only inclusive inputs. In the central and right panels, $\varepsilon_K = |\varepsilon|$ where ε is defined in eq. (16).*

highlights the inclusive-vs-exclusive tensions already discussed by the **UT***fit* collaboration since 2006 [71]. In the same figure the allowed two-dimensional (2D) region, eq.(14), calculated with a 2D procedure inspired by the skeptical method of Ref. [51] with $\sigma = 1$ and denoted as **UT***fit* average, is shown in the plot. The allowed region, as determined by the global fit and denoted as global SM **UT***fit* is also given there. The global fit strongly prefers a value of $|V_{cb}|$ close to its value from inclusive decays and a value of $|V_{ub}|$ close to its exclusive value. This results find a further support by the values denoted as **UT***fit* predictions shown in the fourth column of table I.

III. CP VIOLATION IN THE K^0-$\overline{K^0}$ SYSTEM: ε AND ε'/ε

In this section we discuss an update in the theoretical evaluation of ε and the inclusion, for the first time in the UTA analysis, of the ratio ε'/ε [36]. Although the latter still suffers from large uncertainties, its determination is a very important step in our understanding of CP violation in the SM.

A. An updated evaluation of ε

The parameter ε, which describes indirect CP-violation in the $K^0 - \overline{K}^0$ system, represents one of the most interesting observables in Flavor Physics. It plays an important role in the UTA both within the SM and beyond, see [1]-[2] and references therein. As the phenomenon of $K^0 - \overline{K}^0$ mixing is a loop process further suppressed by the GIM mechanism, ε turns out to be a powerful constraint on New Physics models, for which it is important to have experimental and theoretical uncertainties well under control.

The standard formula for the evaluation of ε is the following

$$\varepsilon = e^{i\,\phi_\varepsilon}\,\sin\phi_\varepsilon\,\left(\frac{\mathrm{Im}M_{12}}{\Delta m_K} + \xi_0\right)\,, \tag{16}$$

where $\xi_0 = \mathrm{Im}A_0/\mathrm{Re}A_0$. At the leading order in the expansion in inverse powers of the charm mass, m_c, $\mathrm{Im}M_{12}$ is given by

$$\begin{aligned}\mathrm{Im}M_{12} = \langle\overline{K}^0|H^{\mathrm{eff}}|K^0\rangle = \frac{G_F^2}{16\,\pi^2}\,M_W^2\,\left[\mathrm{Im}\left(\lambda_c^2\right)\,\left(\eta_1 S_0(x_c) - \eta_3 S_0(x_c,x_t)\right) + \right.\\ \left. +\mathrm{Im}\left(\lambda_t^2\right)\,\left(\eta_2 S_0(x_t) - \eta_3 S_0(x_c,x_t)\right)\right]\,\frac{8}{3}\,f_K^2\,M_K^2\,\hat{B}_K\,,\end{aligned} \tag{17}$$

where $\lambda_i = V_{id}V_{is}^*$; the S_0's are the Inami-Lim functions computed by matching full and effective amplitudes for external states of four quarks with zero momentum [72]; the η_i are the corrections to the Wilson coefficient of the four-fermion operator $Q = \bar{s}\gamma_L^\mu d\;\bar{s}\gamma_L^\mu d$ (in squared parentheses in Eq. (17)), computed at short distance in perturbative

QCD in order to match the Standard Model to the effective Hamiltonian and $\hat{B}_K$ is the renormalisation group invariant bag parameter of the four-fermion operator.

We wish to note that the UTfit Collaboration always computed the Wilson coefficient by evaluating all the η_i simultaneously event by event so that the reduction of the uncertainty noted in [73] was always automatic and active in our calculations.

On the one hand ε is experimentally measured with a 0.4% accuracy, $\varepsilon_K^{\rm exp} = |\varepsilon^{\rm exp}| = 2.228(11) \times 10^{-3}$ [38], on the other hand the theoretical accuracy of the SM prediction is approaching a few percent level, mainly thanks to the improvement of the lattice determination of the relevant bag parameter $\hat{B}_K$ [39],

$$N_f = 2+1 \qquad \hat{B}_K = 0.7625\,(97)\,, \qquad\qquad N_f = 2+1+1 \qquad \hat{B}_K = 0.717\,(18)(16)\,. \tag{18}$$

Following our general approach we average the above two numbers using the PDG method [38] and use

$$\hat{B}_K = 0.756\,(16)\,. \tag{19}$$

Given the improved accuracy, the ξ_0 term and the deviation of the phase ϕ_ε from 45° appearing in Eq. (16) are not negligible [74].

For what concerns ${\rm Im}M_{12}$, the calculation of the amplitude, including long distance contributions, is possible from first principles in lattice QCD [75, 76]. This was also attempted numerically [77] but, for the time being, the difficulty in making the calculation at the physical point in the light quark masses and the extrapolation to the continuum limit, leave too large uncertainties to compete with the standard approach of Eq. (17).

Within the standard approach, the dominant long-distance corrections of $O(1/m_c^2)$ to ${\rm Im}M_{12}$, δ_{BGI} below, due to the exchange of two pions, were evaluated in [78]. The inclusion of this correction and of the more accurate values of ξ_0 and ϕ_ε reduces by 6% the predicted central value of ε. Given the increasing precision of the theoretical ingredients entering ε, it is then becoming important to include all terms expected to contribute to the theoretical evaluation of ε at the percent level. Very recently, in ref. [37], other power corrections due to the finite value of the charm quark mass, denoted as δ_{m_c} below, coming from dimension-8 operators in the effective Hamiltonian were evaluated. We have also included the electroweak corrections, computed in ref. [79], to the charm-top contribution to the coefficient function of the operator Q defined above, denoted as $\delta_{\rm EW}$. By consistency, the electroweak corrections to the renormalisation of the operator Q should be included but this calculation is not available yet.

Up to higher order terms, we may then write

$${\rm Im}M_{12} = \langle \bar{K}^0 | H^{\rm eff} | K^0 \rangle \; (1 + \delta_{\rm EW} + \delta_{BGI} + \delta_{m_c})\;, \tag{20}$$

where $\delta_{BGI} = 0.02$ and the δ_{m_c} correction increases the theoretical prediction for ε_K by 1%. The electroweak correction is $\delta_{\rm EW} \sim 0.15\%$. Both $\delta_{\rm EW}$ and δ_{m_c} are small corrections which are unable to remove the small tension, corresponding to a pull of -1.56, between the UTA theoretical prediction for ε

$$\varepsilon_K = |\varepsilon| = 2.00(15) \times 10^{-3}\,, \tag{21}$$

and the experimental result. From the UTA analysis within the SM, the comparison of the experimental value of ε_K with the theoretical prediction in Eq. (20) allows the extraction of a value of $\hat{B}_K$ that can be compared to the result of lattice calculations. This value is given in subsection IV B, where the corresponding pull is also presented.

Another improvement producing a 2% reduction of the central value is the inclusion of the available NNLO QCD corrections to the Wilson coefficients of the $\Delta S = 2$ effective Hamiltonian [80, 81]. We have not included these corrections, however, since the relevant matrix element, $\hat{B}_K$, computed on the lattice is matched to the $\overline{\rm MS}$ coefficient at the NLO only. In this respect, the perturbative calculation of the NNLO matching of $\hat{B}_K$ from the non-perturbative RI-MOM/SMOM schemes used in lattice calculations to the $\overline{\rm MS}$ scheme would be welcome.

B. New: the lattice determination of ε'/ε

Since this is the first time that ε'/ε is included in the UTA, in this subsection we give some details of its calculation. Our theoretical prediction has been obtained by using the operator matrix elements computed on the lattice by the RBC-UKQCD collaboration [36] and the Wilson coefficients computed with the parameters used in the present work. The calculation requires several steps: i) the evaluation of the matrix elements of the bare lattice four fermion operators in lattice QCD; ii) the matching of the matrix elements of the bare operators to those of the operators renormalised non-perturbatively in some version of the RI-MOM scheme [82], which in ref. [36] was either in the RI-SMOM($\not{q},\not{q}$) or in the RI-SMOM(γ^μ,γ^μ) schemes [83]; iii) the matching of the renormalised operators in the SMOM schemes to

the operators renormalised in the $\overline{\rm MS}$ scheme in which the Wilson coefficient functions have been computed at the NLO [84–87]; iv) the combination of the operators in the $\overline{\rm MS}$ scheme and the Wilson coefficients computed at the NLO to compute the relevant amplitudes. In our analysis we take the matrix elements in the SMOM scheme from ref. [36] and perform the steps iii) and iv) using the parameters extracted in our UTA run.

The expression of ε'/ε is given by

$$\mathrm{Re}\left(\frac{\varepsilon'}{\varepsilon}\right) = -\frac{\omega \sin(\delta_2 - \delta_0 - \phi_\varepsilon)}{\sqrt{2}|\varepsilon|}\left(\frac{\mathrm{Im}A_2}{\mathrm{Re}A_2} - \frac{\mathrm{Im}A_0}{\mathrm{Re}A_0}\left(1 - \hat{\Omega}_{\rm eff}\right)\right), \tag{22}$$

where the isospin breaking effects (both from the mass difference $m_d - m_u$ and from electromagnetic corrections) are encoded in the parameter $\hat{\Omega}_{\rm eff}$. Since at present there is no lattice calculation of this parameter, in this UTA analysis, from the estimate of ref. [88] namely $\hat{\Omega}_{\rm eff} = 17.0^{+9.1}_{-9.0} \cdot 10^{-2}$, by taking a symmetric error, we have used $\hat{\Omega}_{\rm eff} = 17.05(9.05) \cdot 10^{-2}$. In the calculation of ε'/ε we use the experimental value of the parameters ω, δ_2, δ_0, ϕ_ε and $\varepsilon_K = |\varepsilon|$. For comparison with the experimental data, the theoretical values of $\delta_{0,2}(s)$ in the fourth column of the table have been taken from ref. [41] whereas the value of ε_K is extracted from this **UT***fit* analysis. $\mathrm{Re}\,(A_2)$ is extracted from the $K^+ \to \pi^+\pi^0$ decay width; $\mathrm{Re}\,(A_0)$ is computed using the $K^0 \to \pi^+\pi^-$ and $K^0 \to \pi^0\pi^0$ decay widths. To get A_0 from the corresponding decay amplitudes, one takes $x = |A_2|/|A_0| \sim \mathrm{Re}\,(A_2)\,/\mathrm{Re}\,(A_0)$ as a small parameter (its value is about 0.05) and expands the amplitudes to leading order in this parameter. The values of $\mathrm{Re}A_{0,2}$ extracted as explained above are given in table I, the values of $\mathrm{Im}A_{0,2}$ are computed using the matrix elements of the RBC/UKQCD Collaboration [36]. The evaluation of ε'/ε is much harder due to the presence of large cancellations among the contribution of the different operators, particularly between the matrix elements of Q_6 and Q_8 defined below.

The general expression of the amplitude relative to a given isospin channel (in the case of the $K \to \pi\pi$, either $I = 0$ or $I = 2$) in the SM is given by

$$A_{0,2} = \frac{G_F}{\sqrt{2}} V_{us}^* V_{ud} \sum_{i=1}^{10} \left(z_i^{\overline{\rm MS}}(\mu) + \tau y_i^{\overline{\rm MS}}(\mu)\right) M_i^{\overline{\rm MS}}(\mu)_{I=0,2}\,, \tag{23}$$

where the Wilson coefficients z_i, y_i, the matrix elements of the relevant renormalised operators, $M_i^{\overline{\rm MS}}(\mu)_{I=0,2} = \langle\pi\pi|Q_i(\mu)|K\rangle_{I=0,2}$, and $\tau = -V_{ts}^* V_{td}/V_{us}^* V_{ud}$ will be discussed in the following.

1. Operators, bases and matrix elements of bare lattice operators

The bare lattice operators which have been evaluated by the authors of ref. [36] are the following:

- **Current-Current Operators**:

$$Q_1 = (\bar{s}_i\gamma^\mu P_L u_j)(\bar{u}_j\gamma_\mu P_L d_i)\,, \qquad Q_2 = (\bar{s}\gamma^\mu P_L u)(\bar{u}\gamma_\mu P_L d)\,; \tag{24}$$

- **QCD-Penguins Operators**

$$\begin{aligned} Q_3 &= (\bar{s}\gamma^\mu P_L d)\sum_q(\bar{q}\gamma_\mu P_L q)\,, & Q_4 &= (\bar{s}_i\gamma^\mu P_L d_j)\sum_q(\bar{q}_j\gamma_\mu P_L q_i) \\ Q_5 &= (\bar{s}\gamma^\mu P_L d)\sum_q(\bar{q}\gamma_\mu P_R q)\,, & Q_6 &= (\bar{s}_i\gamma^\mu d_j)\sum_q(\bar{q}_j\gamma_\mu P_R q_i)\,; \end{aligned} \tag{25}$$

- **Electroweak-Penguins Operators**

$$\begin{aligned} Q_7 &= \frac{3}{2}(\bar{s}\gamma^\mu P_L d)\sum_q e_q(\bar{q}\gamma_\mu P_R q)\,, & Q_8 &= \frac{3}{2}(\bar{s}_i\gamma^\mu P_L d_j)\sum_q e_q(\bar{q}_j\gamma_\mu P_R q_i) \\ Q_9 &= \frac{3}{2}(\bar{s}\gamma^\mu P_L d)\sum_q e_q(\bar{q}\gamma_\mu P_L q)\,, & Q_{10} &= \frac{3}{2}(\bar{s}_i\gamma^\mu d_j)\sum_q e_q(\bar{q}_j\gamma_\mu P_L q_i)\,, \end{aligned} \tag{26}$$

i	$M_i^{(\not{q},\not{q})}(\mu_0)_{I=0}$ $\left(\mathrm{GeV}^3\right)$	i	$M_i^{(\not{q},\not{q})}(\mu_2)_{I=2}$ $\left(\mathrm{GeV}^3\right)$
1	0.060(39)	(27,1)	0.0506 (29)
2	−0.125(19)	–	–
3	0.142(17)	–	–
5	−0.351(62)	–	–
6	−1.306(90)	–	–
7	0.775(23)	(8,8)	1.003 (0.037)
8	3.312(63)	(8,8)mx	4.43 (18)

TABLE VI. *Physical, extrapolated to the infinite-volume, matrix elements in the RI-SMOM($\not{q},\not{q}$) scheme at $\mu_0 = 4\,GeV$ and $\mu_2 = 3\,GeV$*

where $P_{L/R} = (1 \mp \gamma_5)/2$ are the chiral projectors and e_q is the quark charge in units of e. This basis is used in lattice calculations. For renormalization, however, the chiral basis is better suited for the task since, in the usual 10-operator basis, the operators are not linearly independent. In fact, by Fierz transforming the operators Q_1, Q_2 and Q_3, we define

$$\tilde{Q}_1 = (\bar{s}\gamma^\mu P_L d)(\bar{u}\gamma_\mu P_L u)\,, \qquad \tilde{Q}_2 = (\bar{s}_i\gamma^\mu P_L d_j)(\bar{u}_j\gamma_\mu P_L u_i)\,, \qquad \tilde{Q}_3 = \sum_q (\bar{s}_i\gamma^\mu P_L q_j)(\bar{q}_j\gamma_\mu P_L d_i)$$

we can eliminate operators Q_4, Q_9 and Q_{10} using the relations

$$Q_4 = \tilde{Q}_2 + \tilde{Q}_3 - Q_1\,, \qquad Q_9 = \frac{3}{2}\tilde{Q}_1 - \frac{1}{2}Q_3\,, \qquad Q_{10} = \frac{1}{2}(Q_1 - \tilde{Q}_3) + \tilde{Q}_2\,.$$

The remaining seven operators can then be recombined according to irreducible representations of the chiral flavour-symmetry group $SU(3)_L \otimes SU(3)_R$. The details of the decomposition can be found in [89]. The chiral operator basis, which we will indicate by primed operators, is thus given by

$$\begin{aligned}
&(27,1) \qquad Q'_1 = 3\tilde{Q}_1 + 2Q_2 - Q_3,\\
&(8,1) \quad Q'_2 = \tfrac{1}{5}(2\tilde{Q}_1 - 2Q_2 + Q_3),\\
&(8,1) \quad Q'_3 = \tfrac{1}{5}(-3\tilde{Q}_1 + 3Q_2 + Q_3),\\
&(8,1) \qquad Q'_{5,6} = Q_{5,6},\\
&(8,8) \qquad Q'_{7,8} = Q_{7,8}
\end{aligned} \tag{27}$$

where (L,R) denotes the respective irreducible representations of $SU(3)_L \otimes SU(3)_R$. We recall that the bare lattice matrix elements are converted to the chiral basis by a specific minimization procedure based on the fact that the Fierz identities are not obeyed exactly by the bare lattice matrix elements, for details see ref. [36]. The resulting matrix elements converted back to the 10 operator basis and renormalised in RI-SMOM($\not{q},\not{q}$) are given in table VI (second column).

The operator $(27,1)$ renormalises multiplicatively and contributes to the $I = 2$ channel only, the operators $Q_{7,8}$ mix only among themselves and thus all the $(8,1)$ operators.

For the calculation of A_2 the authors of ref. [41] used the following operator basis

$$\begin{aligned}
Q_{(27,1)} &= (\bar{s}_a\gamma^\mu(1-\gamma_5)d_a)(\bar{u}_b\gamma_\mu(1-\gamma_5)u_b - \bar{d}_b\gamma_\mu(1-\gamma_5)d_b) + (\bar{s}_a\gamma^\mu(1-\gamma_5)u_a)(\bar{u}_b\gamma_\mu(1-\gamma_5)d_b)\,,\\
Q_{(8,8)} &= (\bar{s}_a\gamma^\mu(1-\gamma_5)d_a)(\bar{u}_b\gamma_\mu(1+\gamma_5)u_b - \bar{d}_b\gamma_\mu(1+\gamma_5)d_b) + (\bar{s}_a\gamma^\mu(1-\gamma_5)u_a)(\bar{u}_b\gamma_\mu(1+\gamma_5)d_b)\,,\\
Q_{(8,8)mx} &= (\bar{s}_a\gamma^\mu(1-\gamma_5)d_b)(\bar{u}_b\gamma_\mu(1+\gamma_5)u_a - \bar{d}_b\gamma_\mu(1+\gamma_5)d_a) + (\bar{s}_a\gamma^\mu(1-\gamma_5)u_b)(\bar{u}_b\gamma_\mu(1+\gamma_5)d_a)\,,
\end{aligned} \tag{28}$$

where a, b are summed colour indices. The values of their matrix elements, renormalised in RI-SMOM($\not{q},\not{q}$) , are given in the fourth column of table VI.

2. *Non-perturbative renormalization of lattice matrix elements*

The matrix elements of the bare operators computed on lattice are matched non-perturbatively to a RI-MOM scheme to reduce the uncertainties related to lattice QCD perturbation theory [82]. Since the Wilson coefficients are

Σ_{ij}	Q_1	Q_2	Q_3	Q_5	Q_6	Q_7	Q_8
Q_1	0.001516	5.385×10^{-5}	-9.167×10^{-5}	0.0001252	−0.0003965	0.0004930	0.0007192
Q_2	5.385×10^{-5}	0.0003563	-4.099×10^{-5}	0.0007596	0.0002981	2.914×10^{-5}	−0.0002118
Q_3	-9.167×10^{-5}	-4.099×10^{-5}	0.0002808	0.0003784	0.0004679	-4.656×10^{-5}	0.0001516
Q_5	0.0001252	0.0007596	0.0003784	0.003904	0.001679	-8.000×10^{-5}	−0.0004013
Q_6	−0.0003965	0.0002981	0.0004679	0.001679	0.008188	−0.0003817	−0.002110
Q_7	0.0004930	2.914×10^{-5}	-4.656×10^{-5}	-8.000×10^{-5}	−0.0003817	0.0005395	0.0009460
Q_8	0.0007192	−0.0002118	0.0001516	−0.0004013	−0.002110	0.0009460	0.003937

TABLE VII. *The 7×7 covariance matrix between the renormalized, infinite-volume matrix elements in the RI-SMOM($\not{q}, \not{q}$) scheme in the chiral basis.*

usually given in the $\overline{\text{MS}}$ scheme, we have then to translate the matrix elements to this scheme. This is done by converting the bare lattice matrix elements to the RI-SMOM scheme and then matching at NLO in perturbation theory the result to $\overline{\text{MS}}$.

The authors of refs. [36] and [41] computed the matrix elements either in the RI-SMOM($\not{q}, \not{q}$) or in the RI-SMOM(γ^μ, γ^μ) schemes but used only the results in RI-SMOM($\not{q}, \not{q}$) . According to their choice, in the following, we give only the information necessary for the generation of the UTA events using the matrix elements computed in this scheme. In refs. [36] and [41] the calculations were presented, however, at two different renormalisation scales: for A_2 they used $\mu_2 = 3\,\text{GeV}$ whereas for A_0 the renormalisation scale was $\mu_0 = 4\,\text{GeV}$.

The conversion from the bare lattice matrix elements to those of the RI-SMOM scheme is operated by a matrix $Z_{ij}^{\text{RI}\leftarrow\text{lat}}(\mu_I \text{ GeV})$ according to the relation

$$M_i'^{\,\text{RI}}(\mu_I \text{ GeV})_{I=0,2} = \sum_j Z_{ij}^{\text{RI}\leftarrow\text{lat}}(\mu_I \text{ GeV}) \left(a^{-3} F_I M_j'^{\,\text{lat}}\right)_{I=0,2} \tag{29}$$

where a^{-1} is the inverse of the lattice spacing and F_I is the Lellouch-Lüscher factor accounting for leading finite-volume corrections to the lattice matrix elements in the isospin $I = 0, 2$ channels. We do not need this matrix in our analysis, it can be found in the original publication quoted above.

Once we have the operators in the 7-operator basis, we can perform the non-perturbative renormalization using a 7×7 renormalization matrix. In the case of A_0, the matrix elements in 7-operator basis at renormalization scale of $\mu = 4$ GeV in the RI-SMOM($\not{q}, \not{q}$) scheme, and the corresponding covariance matrix, $\Sigma_{ij} = \rho_{ij}\sigma_i\sigma_j$, are given in table VI and VII respectively; ρ_{ij} is the correlation matrix and σ_i are the errors associated to the matrix elements. In the case of A_2 it was not possible to obtain the correlation matrix from the authors. To be conservative in the evaluation of the uncertainties we considered three cases: a) no correlation among the three operators of eq. (28); b) maximal correlation, namely $\rho_{ij} = 1$, and c) the same correlation for the operators mediating $\Delta I = 3/2$ transitions as the one computed for $\Delta I = 1/2$ transitions in ref. [36]. In the latter case the correlation matrix can be easily derived using the covariance matrix given in Table VII. The difference between the results obtained with a)-c) is tiny with respect to the overall uncertainty and was absorbed in the overall uncertainty.

At this point one matches the RI-SMOM($\not{q}, \not{q}$) renormalized matrix elements to the $\overline{\text{MS}}$ scheme. This is done with another renormalization matrix $Z_{ij}^{\overline{\text{MS}}\leftarrow\text{RI}}(\mu)$ that is found in ref. [89]

$$Z_{ij}^{\overline{\text{MS}}\leftarrow\text{RI}}(\mu) = \delta_{ij} + \frac{\alpha_s(\mu)}{4\pi} \Delta r_{ij}^{\overline{\text{MS}}\leftarrow\text{RI}}\,. \tag{30}$$

The non-zero matrix elements for the $\Delta r_{ij}^{\overline{\text{MS}}\leftarrow\text{RI}}$ matrix of eq. (30) are, in the case of the matching between the RI-SMOM($\not{q}, \not{q}$) and $\overline{\text{MS}}$ schemes given in Table VIII, where the gauge parameter is denoted by ξ_G ($\xi_G = 0, 1$ correspond to the Landau and Feynman gauges, respectively). In our case the appropriate value is $\xi_G = 0$.

3. Wilson coefficients and final result

After the conversion of the matrix elements in the $\overline{\text{MS}}$ scheme, we can compute the A_0 and A_2 amplitudes using eq. (23). The expression of the Wilson coefficients z_i, y_i can be found at NLO in the references [84–87].

From the UTA we find

$$\tau = -\frac{V_{ts}^* V_{td}}{V_{us}^* V_{ud}} = 0.001482(36) - i\,0.000644(16)\,. \tag{31}$$

(i,j)	$\Delta r_{ij}^{\overline{\rm MS}\leftarrow{\rm RI}}$
(1,1)	$\xi_G\left(\frac{C_0}{N_c} - C_0 - \frac{4\log(2)}{N_c} + 4\log(2)\right) - \frac{12\log(2)}{N_c} + 12\log(2) + \frac{9}{N_c} - 9$
(2,2)	$\xi_G\left(\frac{4C_0N_c}{5} + \frac{C_0}{N_c} - \frac{6C_0}{5} - \frac{4\log(2)}{N_c} - \frac{4N_c}{5} + \frac{6}{5}\right) - \frac{12\log(2)}{N_c} + \frac{8N_c}{5} + \frac{9}{N_c} - \frac{12}{5}$
(2,3)	$\xi_G\left(\frac{6C_0N_c}{5} - \frac{9C_0}{5} + 4\log(2) - \frac{6N_c}{5} + \frac{4}{5}\right) + 12\log(2) + \frac{12N_c}{5} - \frac{53}{5}$
(3,2)	$\xi_G\left(-\frac{6C_0N_c}{5} + \frac{4C_0}{5} + 4\log(2) + \frac{6N_c}{5} - \frac{9}{5}\right) + 12\log(2) - \frac{12N_c}{5} + \frac{2}{3N_c} - \frac{263}{45}$
(3,3)	$\xi_G\left(-\frac{9C_0N_c}{5} + \frac{C_0}{N_c} + \frac{6C_0}{5} - \frac{4\log(2)}{N_c} + \frac{9N_c}{5} - \frac{6}{5}\right) - \frac{12\log(2)}{N_c} - \frac{18N_c}{5} + \frac{85}{9N_c} + \frac{26}{15}$
(3,5)	$\frac{2}{9N_c}$
(3,6)	$-\frac{2}{9}$
(5,5)	$\xi_G\left(\frac{C_0}{2N_c} - \frac{2\log(2)}{N_c} - \frac{1}{2N_c}\right) + \frac{3C_0}{2N_c} - \frac{2\log(2)}{N_c} - \frac{2}{N_c}$
(5,6)	$\xi_G\left(-\frac{C_0}{2} + 2\log(2) + \frac{1}{2}\right) - \frac{3C_0}{2} + 2\log(2) + 2$
(6,2)	$\frac{5}{N_c} - \frac{10}{3}$
(6,3)	$\frac{10}{3N_c} - 5$
(6,5)	$\left(2\log(2) - \frac{1}{2}\right)\xi_G + 2\log(2) + \frac{5}{3N_c} - 2$
(6,6)	$\xi_G\left(-\frac{C_0N_c}{2} + \frac{C_0}{2N_c} - \frac{2\log(2)}{N_c} + N_c - \frac{1}{2N_c}\right) - \frac{3C_0N_c}{2} + \frac{3C_0}{2N_c} - \frac{2\log(2)}{N_c} + 4N_c - \frac{2}{N_c} - \frac{5}{3}$
(7,7)	$\xi_G\left(\frac{C_0}{2N_c} - \frac{2\log(2)}{N_c} - \frac{1}{2N_c}\right) + \frac{3C_0}{2N_c} - \frac{2\log(2)}{N_c} - \frac{2}{N_c}$
(7,8)	$\xi_G\left(-\frac{C_0}{2} + 2\log(2) + \frac{1}{2}\right) - \frac{3C_0}{2} + 2\log(2) + 2$
(8,7)	$\left(2\log(2) - \frac{1}{2}\right)\xi_G + 2\log(2) - 2$
(8,8)	$\xi_G\left(-\frac{C_0N_c}{2} + \frac{C_0}{2N_c} - \frac{2\log(2)}{N_c} + N_c - \frac{1}{2N_c}\right) - \frac{3C_0N_c}{2} + \frac{3C_0}{2N_c} - \frac{2\log(2)}{N_c} + 4N_c - \frac{2}{N_c}$

TABLE VIII. *Non-zero matrix elements for the $\Delta r_{ij}^{\overline{MS}\leftarrow RI}$ matrix of eq. (30) are shown in the case of the matching between the RI-SMOM($\not{q},\not{q}$) and $\overline{MS}$ schemes. $C_0 = 2/3\Psi'(1/3) - (2\pi/3)^2 \sim 2.34391$, where Ψ is the digamma function.*

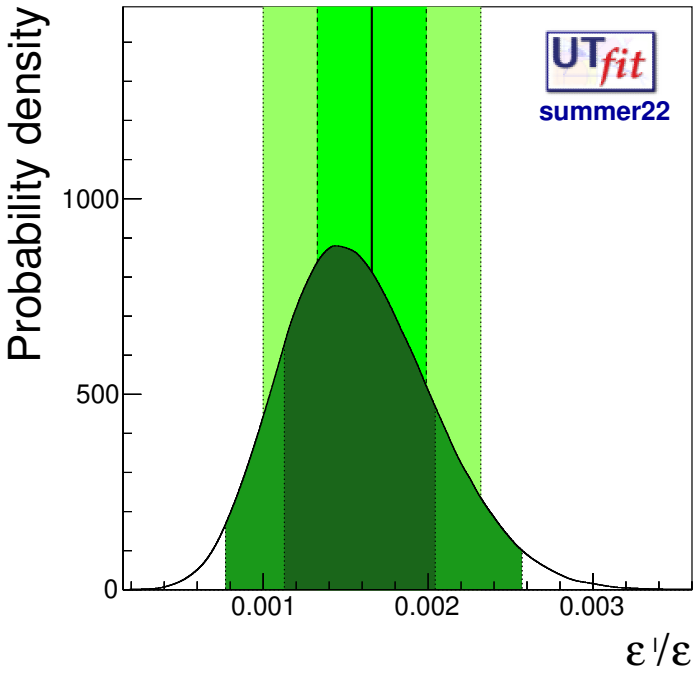

FIG. 2. *The prediction of ε'/ε obtained within this UT analysis. The vertical band represents the experimental measurement and uncertainty of this quantity.*

The values of the generated amplitudes $\mathrm{Re}\,(A_0)$ and $\mathrm{Re}\,(A_2)$ are given in table I.We also find $\mathrm{Im}\,(A_0) = -6.75(86) \times 10^{-11}$ GeV and $\mathrm{Im}\,(A_2) = -8.4(1.2) \times 10^{-13}$ GeV. For the calculation of ε'/ε, however, assuming the validity of the SM, the real part of these amplitudes are taken from the experiments in order to reduce the final theoretical uncertainty. For this quantity we get

$$\varepsilon'/\varepsilon = 15.2(4.7) \cdot 10^{-4}\,. \tag{32}$$

This number can be compared with the RBC/UKQCD result, given without error, which includes the isospin breaking corrections of ref. [88], $\varepsilon'/\varepsilon = 16.7 \cdot 10^{-4}$ (RBC/UKQCD quotes $21.7(8.4) \cdot 10^{-4}$ without isospin breaking corrections), and with the experimental value $\varepsilon'/\varepsilon = 16.6(3.3) \cdot 10^{-4}$. The predicted distribution of ε'/ε is shown in Fig. 2. Within still large theoretical uncertainties the SM predictions and experimental results are in very good agreement and there is no sign of NP. The novelty here is the insertion of the determination of ε'/ε in the full UT analysis.

C. The Unitarity Triangle angles

For what concerns the values of the Unitarity Triangle angles, we used the following inputs:

- β (or ϕ_1): the value of sin β is taken from the latest HFLAV average [22] with the most updated inputs, which gives $\sin 2\beta = 0.688(20)$. We then add a correction factor of $-0.01(1)$, although strictly speaking this applies exclusively to the $J/\psi\, K^0$ channel, as data-driven theory uncertainty obtained with the method described in ref. [90];
- α (or ϕ_2): the value of the angle α is obtained by UTfit isospin analyses of the three contributing final states $\pi\pi$, $\rho\rho$ and $\rho\pi$. The various probability distributions are shown in Fig. 3 (left panel) together with the combined one that is used as input to our global fit;
- γ (or ϕ_3): the value of the angle γ is taken from the latest HFLAV average [22] and the corresponding probability distribution is shown in Fig. 3 (right panel) together with the prediction from the global fit.

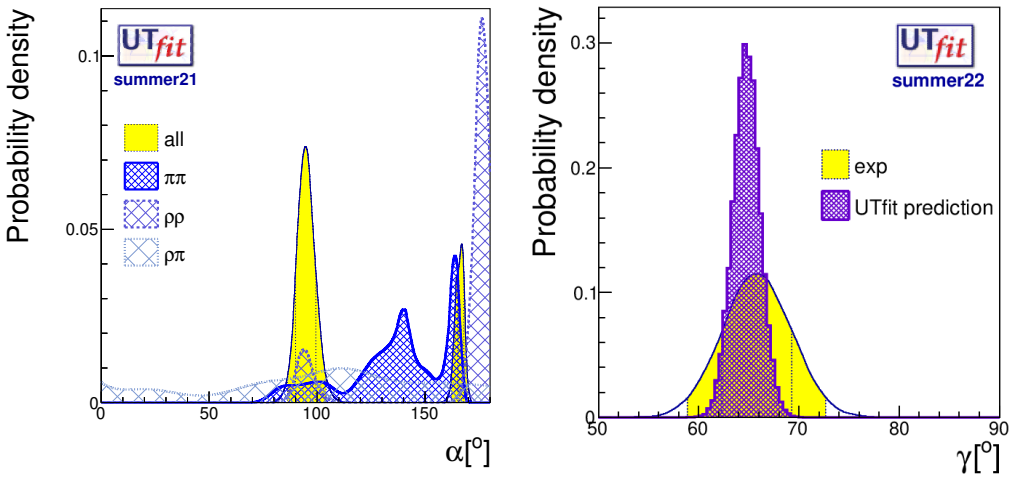

FIG. 3. *Left: global fit input distribution for the angle α (in solid yellow histogram) with the three separate distributions coming from the three contributing final states $\pi\pi$, $\rho\rho$ and $\rho\pi$; Right: global fit input distribution for the angle γ (in solid yellow histogram) obtained by the HFLAV [22] average compared with the global* **UT***fit prediction for the same angle.*

The full list of measurements used as inputs in the global fit is given in the first and second columns of table I. ε, ε'/ε, $|V_{ub}|$ and $|V_{cb}|$ have been discussed in the previous sections.

IV. STANDARD MODEL UNITARITY TRIANGLE ANALYSIS

The results of the global SM fit are given as two-dimensional probability distributions in the plane of the CKM parameters $\bar{\rho}$ and $\bar{\eta}$ and shown in Fig. 4. The numerical results are in Table IX. Besides the global fit shown in the top-left panel, we have studied various configurations which provide us further physical information:

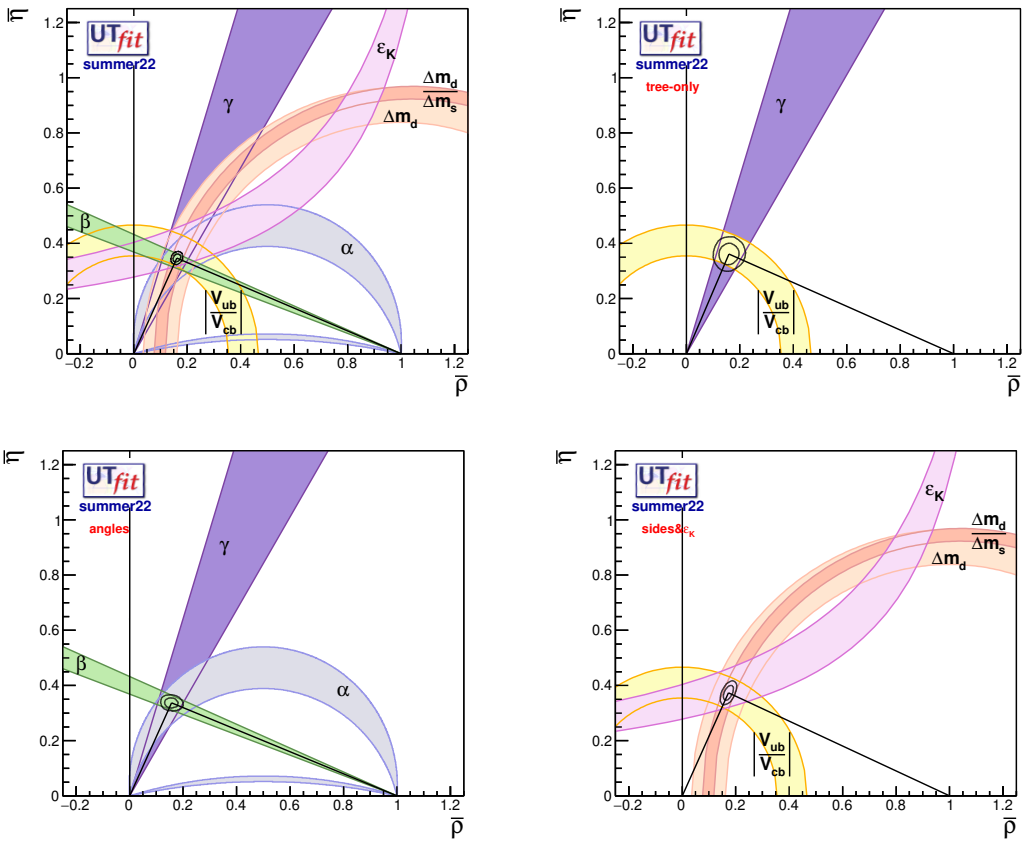

FIG. 4. *$\bar{\rho}$-$\bar{\eta}$ planes with the SM global fit results in various configurations. The black contours display the 68% and 95% probability regions selected by the given global fit. The 95% probability regions selected are also shown for each constraint considered. Top-Left: full SM fit; Top-Right: fit using as inputs the "tree-only" constraints; Bottom-Left: fit using as inputs only the angle measurements; Bottom-Right: fit using as inputs only the side measurements and the mixing parameter ε_K in the kaon system.*

fit configuration	$\bar{\rho}$	$\bar{\eta}$
full SM fit	0.161(10)	0.347(10)
tree-only fit	±0.158(26)	±0.362(27)
angle-only fit	0.156(17)	0.334(12)
no-angles fit	0.157(17)	0.337(12)

TABLE IX. *Results for the $\bar{\rho}$ and $\bar{\eta}$ values as extracted from the various fit configurations. The Universal Unitarity Triangle (UUT) fit includes the three angles inputs and the semileptonic ratio $|V_{ub}/V_{cb}|$ [91].*

1. By fitting the "tree-only" constraints, i.e. processes for which a contribution from new physics is with the highest probability absent, we test the possibility that all the sources of CP violation come from physics beyond the SM. The results shown in the top-right panel, which have a two-fold sign ambiguity in the $\bar{\rho}$-$\bar{\eta}$ values, show that the SM alone contributes to the largest part of the observed CP violation at low energy;

2. We analysed the results that can be obtained by using only the information coming from the measured angles, "angle-only" fit, bottom-left panel;

3. We analysed the results that can be obtained from the triangle sides fit and ε, "sides+ ε_K" fit, bottom-right panel.

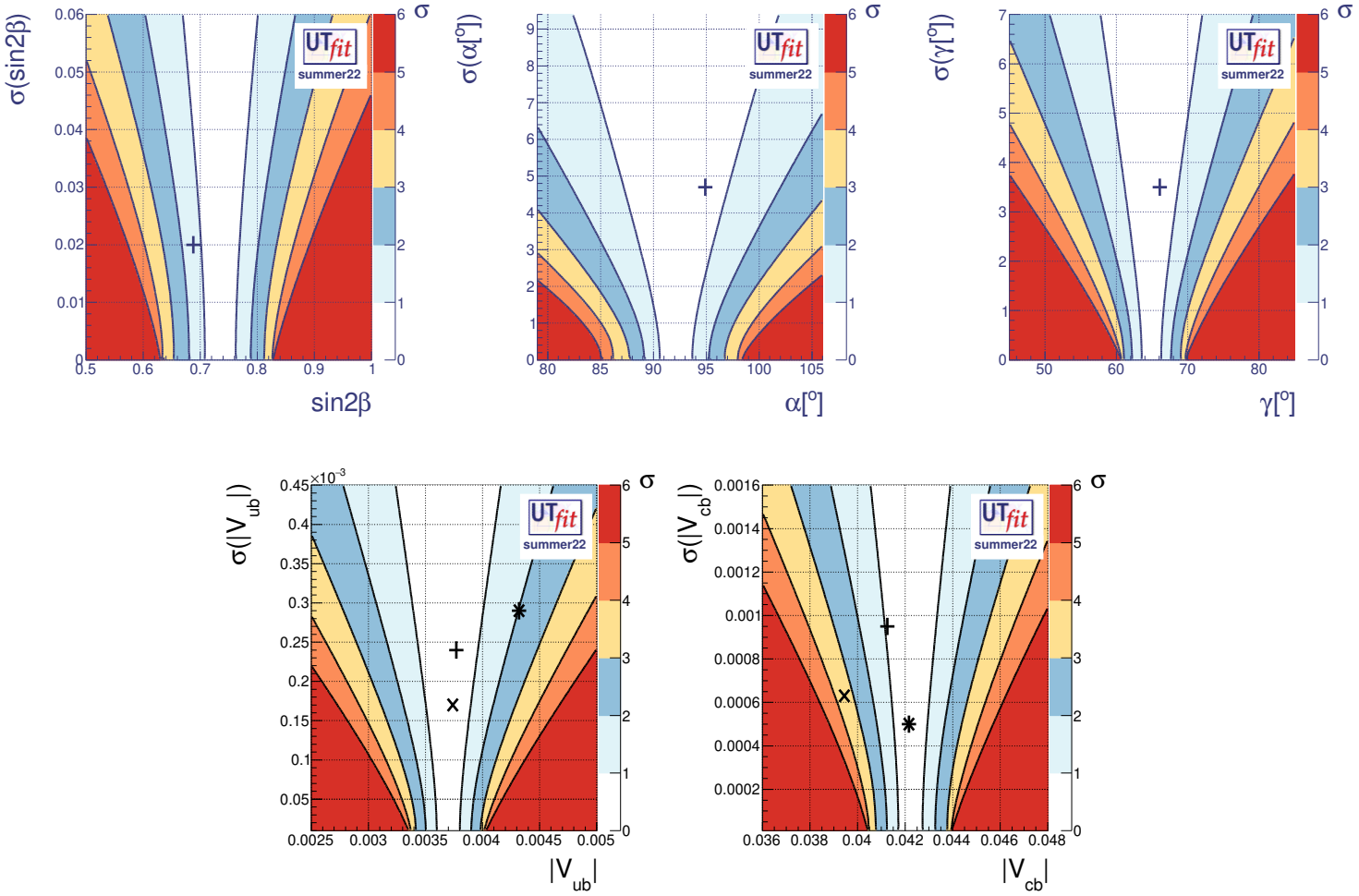

FIG. 5. *Pull plots (see text) for* $\sin 2\beta$ *(top-left),* α *(top-centre),* γ *(top-right),* $|V_{ub}|$ *(bottom-left) and* $|V_{cb}|$ *(bottom-right) inputs. The crosses represent the input values reported in Table I. In the case of* $|V_{ub}|$ *and* $|V_{cb}|$ *the* x *and the* * *represent the values extracted from exclusive and inclusive semileptonic decays respectively.*

We observe that there is not a particular bias from either case forcing the global fit to fill a specific region of the plane, all fits prefer essentially the same region in the $\bar{\rho}$-$\bar{\eta}$ plane. We want also to give the CKM matrix in all its glory

$$V_{\rm CKM} = \begin{pmatrix} 0.97431(19) & 0.22517(81) & 0.003715(93)\, e^{-i(65.1(1.3))^o} \\ -0.22503(83)\, e^{+i(0.0351(1))^o} & 0.97345(20)\, e^{-i(0.00187(5))^o} & 0.0420(5) \\ 0.00859(11)\, e^{-i(22.4(7))^o} & -0.04128(46)\, e^{+i(1.05(3))^o} & 0.999111(20) \end{pmatrix} . \tag{33}$$

From the global fit we also obtain

$$\lambda = 0.22519(83)\,, \qquad \mathcal{A} = 0.828(11)\,. \tag{34}$$

Several other quantities that we have analysed in our fit can be found in Table X and XI in the Appendix.

A. Pull plots and allowed regions

For a given quantity x, the compatibility between its UTA prediction $\bar{x}$, given in Table I, and its direct measurement $\hat{x}$ is obtained integrating the probability density function (pdf) $p(\bar{x} - \hat{x})$, in the region for which it acquires values smaller than $p(0)$, namely the region for which the pdf value is smaller than that of the case $\bar{x} = \hat{x}$, i.e., when the measurement matches the prediction. This two-sided p-value is then converted to the equivalent number of standard deviations for a Gaussian distribution. When $\bar{x} - \hat{x}$ is distributed according to a Gaussian p.d.f, this quantity coincides

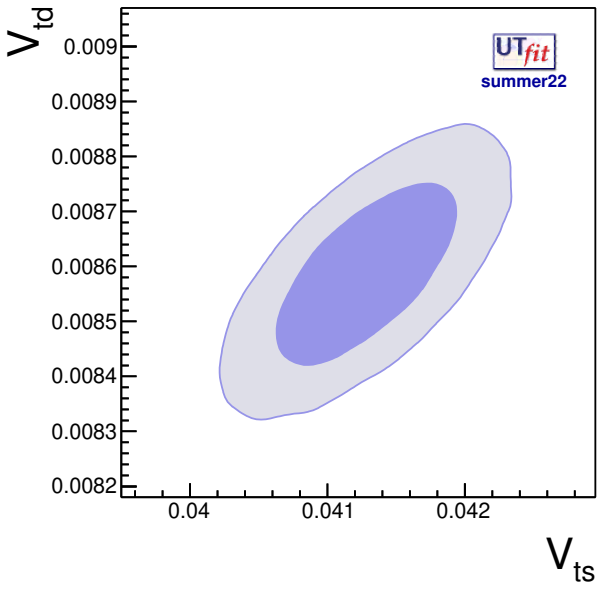

FIG. 6. *Allowed region in the $|V_{td}|$-$|V_{ts}|$ plane.*

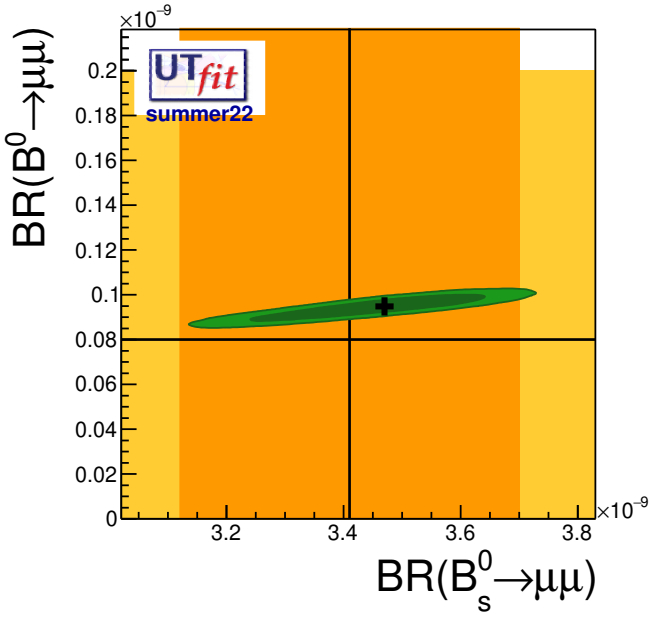

FIG. 7. *Allowed region in the $BR(B_s^0 \to \mu\mu)$-$BR(B^0 \to \mu\mu)$ plane. The vertical (orange) and horizontal (yellow) bands correspond to the present experimental results (1σ regions).*

with the usual pull, i.e. with the ratio between $|\bar{x} - \hat{x}|$ and its standard deviation. The advantage of this approach is that no approximation is made on the shape of pdf's.

The so-called "pull plots" are then constructed assuming a measured value and an experimental error for each point of the plane, with the procedure described above (assuming that the measurement has a Gaussian pdf). In Fig. 5 these plots are used to assess the agreement of a given measurement with the indirect determination from the fit using all the other inputs. The coloured areas represent the level of agreement between the predicted values and the measurements at better than 1, 2, ... $n\,\sigma$. The markers (crosses) have the coordinates (x, y) = (central value, error)

of the direct measurements considered, see Table I. In the case of $|V_{ub}|$ and $|V_{cb}|$ the x and the * represent the values extracted from exclusive and inclusive semileptonic decays respectively. These plots allow to visualise the tensions between each input and the rest of them as in the pull column of Table I. It is clear that inputs as α and γ show very good agreement with the rest of the fit, while $\sin 2\beta$, $|V_{ub}|$ and $|V_{cb}|$ present various degrees of tension either directly or with respect to the different exclusive or inclusive determinations.

Overall, the global fit proves a remarkable internal consistency with a better than 7% precision in the determination of the fundamental CKM parameters $\bar{\rho}$ and $\bar{\eta}$. New physics effects, if present, would give rather small contributions and for this reason it is necessary to improve both the precision of the experiments and the accuracy of the theoretical calculations.

We also find useful to provide some further information coming form our global UT analysis: in Fig. 6 we show the constraint on the third row of the CKM matrix given by the allowed region, mainly determined by neutral B meson mixing, in the $|V_{td}|$-$|V_{ts}|$ plane; in Fig. 7 we show the allowed region in the $BR(B_s^0 \to \mu\mu)$-$BR(B^0 \to \mu\mu)$ plane compared with the experimental measurements given by the vertical (orange) and horizontal (yellow) bands corresponding to the present experimental constraints.

B. Constraints on the lattice parameters in the Standard Model

Assuming the validity of the Standard Model, the constraints in the $\bar{\rho}$-$\bar{\eta}$ plane allow the "experimental" determination of several hadronic quantities which, in the previous fits, were taken from lattice QCD calculations. This approach has the advantage that we can extract from the combined experimental measurements the value of $\hat{B}_K$, of the B^0 mixing amplitudes, $f_{B_{s,d}}\hat{B}^{1/2}_{s,d}$ or $f_{B_s}\hat{B}^{1/2}_s$, and of $\xi = f_{B_s}\hat{B}^{1/2}_s/f_{B_d}\hat{B}^{1/2}_d$. We have considered the following possibilities (the derived lattice quantities and their uncertainties, obtained by combining the lattice inputs of Table III are denoted by "latt.*"):

1. we remove from the lattice inputs $\hat{B}_K$ and we compare the **UT***fit* value with the lattice result

$$\hat{B}_K(\mathbf{UT}fit) = 0.840(59)\,, \qquad \hat{B}_K(\text{latt.}) = 0.756(16)\,; \tag{35}$$

2. we only use $\hat{B}_s$ and $\hat{B}_s/\hat{B}_d$ and derive

$$\begin{aligned} f_{B_d}(\mathbf{UT}fit) &= 190.9(7.2)\,\text{MeV}\,, & f_{B_d}(\text{latt.}*) &= 190.5(1.3)\,\text{MeV}\,; \\ f_{B_s}(\mathbf{UT}fit) &= 229.4(7.2)\,\text{MeV}\,, & f_{B_s}(\text{latt.}*) &= 230.1(1.2)\,\text{MeV}\,; \\ \xi(\mathbf{UT}fit) &= 1.204(27)\,, & \xi(\text{latt.}*) &= 1.208(59)\,; \end{aligned} \tag{36}$$

3. we use only the ratios f_{B_s}/f_{B_d} and $\hat{B}_s/\hat{B}_d$ but not f_{B_s} and $\hat{B}_s$

$$\begin{aligned} f_{B_d}\hat{B}^{1/2}_d(\mathbf{UT}fit) &= 216.9(5.3)\,\text{MeV}\,, & f_{B_d}\hat{B}^{1/2}_d(\text{latt.}*) &= 214.2(5.6)\,\text{MeV}\,; \\ f_{B_s}\hat{B}^{1/2}_s(\mathbf{UT}fit) &= 264.4(6.0)\,\text{MeV}\,, & f_{B_s}\hat{B}^{1/2}_s(\text{latt.}*) &= 260.7(6.1)\,\text{MeV}\,; \\ \xi(\mathbf{UT}fit)) &= 1.219(12)\,, & \xi(\text{latt.}*) &= 1.208(51)\,; \end{aligned} \tag{37}$$

4. we only use $\hat{B}_K$ but not any of the other inputs of table III

$$\begin{aligned} f_{B_d}\hat{B}^{1/2}_d(\mathbf{UT}fit) &= 210.5(3.6)\,\text{MeV}\,, & f_{B_d}\hat{B}^{1/2}_d(\text{latt.}*) &= 214.2(5.6)\,\text{MeV}\,; \\ f_{B_s}\hat{B}^{1/2}_s(\mathbf{UT}fit) &= 259.0(3.4)\,\text{MeV}\,, & f_{B_s}\hat{B}^{1/2}_s(\text{latt.}*) &= 260.7(6.1)\,\text{MeV}\,; \\ \xi(\mathbf{UT}fit) &= 1.230(23)\,, & \xi(\text{latt.}*) &= 1.217(14)\,. \end{aligned} \tag{38}$$

We observe that the case 3. has simply slightly larger uncertainties than the case 4. and that the **UT***fit* predictions of the hadronic parameters are fully compatible with the lattice calculations. For further information, we also repeated the case 1. with $|V_{cb}|$ taken from Eq. (10) instead than Eq. (8) obtaining $B_K(\mathbf{UT}fit) = 0.831(57)$ in substantial agreement with the result in Eq. (35). This remains true for the other parameter condidered in all the other cases (2.-3.-4.).

V. CONCLUSIONS

Our main conclusions are the following:

- The SM analysis shows a very good overall consistency;
- The exclusive vs inclusive saga is not concluded yet although there are signals that it could be quickly resolved. We stress that, as in the past [2], the unitarity triangle analysis, namely the analysis without including the experimental measurements from semileptonic decays, favours a large value of $|V_{cb}|$, close to the inclusive determination, and a smalle value of $|V_{ub}|$, close to the exclusive determination;
- For $|V_{cb}|$, on the theoretical side, there are signals that a more accurate determination of the form factors obtained from new and more accurate lattice calculations and the DM approach [63], combined with a more careful treatment of the experimental data, could increase the central value and determine more realistically the uncertainty, thus reducing substantially the tension between the inclusive and exclusive values of this quantity. The difference with respect to previous analyses is not only due to the use of the DM approach but also to a critical examination of the experimental correlation matrix of the $B \to D^*$ differential decay rates and to the theoretical determination of the momentum dependence of the form factors independently of the experiments and before fitting the data [60–63].
- Similar analyses are needed for semileptonic $B \to \pi$ decays, although in that case the tension is smaller since the uncertainties in both the inclusive and exclusive determinations of $|V_{ub}|$ are larger. In ref. [92] for example, using the DM approach, the results are $|V_{ub}| \times 10^3 = 3.62(47)$ from $B \to \pi$ decays and $|V_{ub}| \times 10^3 = 3.77(48)$ from $B_s \to K$ decays, compatible with the latest inclusive determination $|V_{ub}| \times 10^3 = 4.13(26)$ from PDG [38];
- On the experimental side, regarding the differences between exclusive and inclusive semileptonic B decays, we really need more measurements from LHCb and (mostly) Belle II;
- Most of the quantities studied in this work refer to the quark down sector for which the CKM paradigm has been (and still is) a great success in predicting weak processes (mainly to the physics of strange and beauty particles). Only recently we experimentally started to investigate if there are signals of New Physics in the up sector singled by discrepancies between measurements and theoretical predictions. The discovery of CP violation in neutral D meson system has opened a new sector of investigation and will be the subject of our study in a future publication.

ACKNOWLEDGMENTS

We thank Antonio Di Domenico, C. Kelly and C. Sachrajda for very useful discussions. The work of M.V. is supported by the Simons Foundation under the Simons Bridge for Postdoctoral Fellowships at SCGP and YITP, award number 815892. DD is thankful to HSE basic research program. This work was partly supported by the Italian Ministry of Research (MIUR) under grant PRIN 20172LNEEZL.V. acknowledge the hospitality of the Scuola Normale Superiore and of the INFN, Sezione di Pisa where part of this work was developed.

APPENDIX

Observable	Full Fit	Full Fit (95%)
λ	0.22519 ± 0.00083	$[0.22359, 0.22686]$
$\mathcal{A}$	0.828 ± 0.011	$[0.807, 0.851]$
$\bar{\rho}$	0.1609 ± 0.0095	$[0.1430, 0.1794]$
$\bar{\eta}$	0.347 ± 0.010	$[0.327, 0.367]$
β	22.46 ± 0.68	$[21.13, 23.78]$
α	92.4 ± 1.4	$[89.9, 95.4]$
β_s	-0.0368 ± 0.0010	$[-0.0388, -0.0347]$
$\sin\theta_{12}$	0.22519 ± 0.00083	$[0.22359, 0.22686]$
$\sin\theta_{23}$	0.04200 ± 0.00047	$[0.04109, 0.04290]$
$\sin\theta_{13}$	0.003714 ± 0.000092	$[0.003528, 0.003898]$
$\delta[^\circ]$	1.137 ± 0.022	$[1.092, 1.180]$
$J_{CP} \times 10^5$	3.102 ± 0.080	$[2.946, 3.264]$
R_t	0.9082 ± 0.0084	$[0.8908, 0.9244]$
R_b	0.383 ± 0.011	$[0.362, 0.404]$
$\lvert V_{td}/V_{ts}\rvert$	0.2080 ± 0.0020	$[0.2041, 0.2119]$
$\mathrm{BR}(B_d \to \mu\mu) \times 10^{10}$	0.949 ± 0.037	$[0.871, 1.009]$
$\mathrm{BR}(B_s \to \mu\mu) \times 10^{9}$	3.25 ± 0.12	$[3.01, 3.44]$
$\lvert V_{ud}\rvert$	0.97431 ± 0.00019	$[0.97392, 0.97468]$
$\lvert V_{us}\rvert$	0.22517 ± 0.00081	$[0.22352, 0.22682]$
$\lvert V_{ub}\rvert$	0.003715 ± 0.000093	$[0.003532, 0.003898]$
$\lvert V_{cd}\rvert$	0.22503 ± 0.00083	$[0.22343, 0.22669]$
$\lvert V_{cs}\rvert$	0.97345 ± 0.00020	$[0.97305, 0.97381]$
$\lvert V_{cb}\rvert$	0.04200 ± 0.00047	$[0.04109, 0.04290]$
$\lvert V_{td}\rvert$	0.00859 ± 0.00011	$[0.00837, 0.00880]$
$\lvert V_{ts}\rvert$	0.04128 ± 0.00046	$[0.04038, 0.04217]$
$\lvert V_{tb}\rvert$	0.999111 ± 0.000020	$[0.999072, 0.999149]$

TABLE X. *Extra outputs of interest obtained from our UTA analysis I.*

Observable	Full Fit	Full Fit (95%)
$\mathrm{Re}(\lambda^t_{sd})$	-0.0003252 ± 0.0000080	$[-0.0003413, -0.0003098]$
$\mathrm{Re}(\lambda^c_{sd})$	-0.21908 ± 0.00076	$[-0.22058, -0.21757]$
$\mathrm{Re}(\lambda^u_{sd})$	0.21943 ± 0.00077	$[0.21789, 0.22090]$
$\mathrm{Re}(\lambda^t_{bd})$	0.00794 ± 0.00013	$[0.00769, 0.00818]$
$\mathrm{Re}(\lambda^c_{bd})$	-0.00945 ± 0.00011	$[-0.00967, -0.00924]$
$\mathrm{Re}(\lambda^u_{bd})$	0.001522 ± 0.000090	$[0.001344, 0.001699]$
$\mathrm{Re}(\lambda^t_{bs})$	-0.04123 ± 0.00046	$[-0.04216, -0.04037]$
$\mathrm{Re}(\lambda^c_{bs})$	0.04089 ± 0.00045	$[0.04001, 0.04177]$
$\mathrm{Re}(\lambda^u_{bs})$	-0.04123 ± 0.00046	$[-0.04216, -0.04037]$
$\mathrm{Im}(\lambda^t_{sd}) \times 10^5$	14.13 ± 0.37	$[13.42, 14.85]$
$\mathrm{Im}(\lambda^c_{sd}) \times 10^5$	-14.13 ± 0.37	$[-14.85, -13.42]$
$\mathrm{Im}(\lambda^t_{bd}) \times 10^5$	-327.6 ± 8.1	$[-343.2, -311.3]$
$\mathrm{Im}(\lambda^c_{bd}) \times 10^5$	-0.578 ± 0.018	$[-0.615, -0.545]$
$\mathrm{Im}(\lambda^u_{bd}) \times 10^5$	328.1 ± 8.3	$[311.6, 344.0]$
$\mathrm{Im}(\lambda^t_{bs}) \times 10^5$	-75.7 ± 1.9	$[-79.4, -71.8]$
$\mathrm{Im}(\lambda^c_{bs}) \times 10^5$	-0.1336 ± 0.0041	$[-0.1420, -0.1258]$
$\mathrm{Im}(\lambda^u_{bs}) \times 10^5$	-75.7 ± 1.9	$[-79.4, -71.8]$
$\lvert\lambda^t_{sd}\rvert$	0.0003545 ± 0.0000075	$[0.0003398, 0.0003698]$
$\lvert\lambda^c_{sd}\rvert$	0.21908 ± 0.00076	$[0.21757, 0.22058]$
$\lvert\lambda^u_{sd}\rvert$	0.21943 ± 0.00077	$[0.21789, 0.22090]$
$\lvert\lambda^t_{bd}\rvert$	0.00858 ± 0.00011	$[0.00837, 0.00880]$
$\lvert\lambda^c_{bd}\rvert$	0.00945 ± 0.00011	$[0.00924, 0.00967]$
$\lvert\lambda^u_{bd}\rvert$	0.003618 ± 0.000091	$[0.003436, 0.003794]$
$\lvert\lambda^t_{bs}\rvert$	0.04125 ± 0.00045	$[0.04037, 0.04213]$
$\lvert\lambda^c_{bs}\rvert$	0.04089 ± 0.00045	$[0.04001, 0.04177]$
$\lvert\lambda^u_{bs}\rvert$	0.04125 ± 0.00045	$[0.04037, 0.04213]$
$\mathrm{Im}(\tau)$	-0.000644 ± 0.000016	$[-0.000678, -0.000612]$
$\mathrm{Re}(\tau)$	0.001482 ± 0.000036	$[0.001410, 0.001557]$

TABLE XI. *Extra outputs of interest obtained from our UTA analysis II.* $\lambda^q_{ij} = V_{qi}V^*_{qj}$.

[1] M. Ciuchini, G. D'Agostini, E. Franco, V. Lubicz, G. Martinelli, F. Parodi et al., *2000 CKM triangle analysis: A Critical review with updated experimental inputs and theoretical parameters*, *JHEP* **07** (2001) 013, [hep-ph/0012308].

[2] C. Alpigiani et al., *Unitarity Triangle Analysis in the Standard Model and Beyond*, in *5th Large Hadron Collider Physics Conference*, 10, 2017. 1710.09644.

[3] M. Bona et al., *Unitarity Triangle global fits beyond the Standard Model: UTfit 2021 NP update*, *PoS* **EPS-HEP2021** (2022) 500.

[4] M. Bona et al., *Unitarity Triangle global fits testing the Standard Model: UTfit 2021 SM update*, *PoS* **EPS-HEP2021** (2022) 512.

[5] A. J. Buras, *Standard Model Predictions for Rare K and B Decays without New Physics Infection*, 2209.03968.

[6] N. Cabibbo, *Unitary Symmetry and Leptonic Decays*, *Phys. Rev. Lett.* **10** (1963) 531–533.

[7] M. Kobayashi and T. Maskawa, *CP Violation in the Renormalizable Theory of Weak Interaction*, *Prog. Theor. Phys.* **49** (1973) 652–657.

[8] L. Wolfenstein, *Parametrization of the Kobayashi-Maskawa Matrix*, *Phys. Rev. Lett.* **51** (1983) 1945.

[9] A. J. Buras, M. E. Lautenbacher and G. Ostermaier, *Waiting for the top quark mass,* $K^+ \to \pi^+\nu\bar{\nu}$, $B^0_s - \bar{B}^0_s$ *mixing and CP asymmetries in B decays*, *Phys. Rev. D* **50** (1994) 3433–3446, [hep-ph/9403384].

[10] S. L. Glashow, J. Iliopoulos and L. Maiani, *Weak Interactions with Lepton-Hadron Symmetry*, *Phys. Rev. D* **2** (1970) 1285–1292.

[11] P. Gambino and C. Schwanda, *Inclusive semileptonic fits, heavy quark masses, and* V_{cb}, *Phys. Rev. D* **89** (2014) 014022, [1307.4551].

[12] A. Alberti, P. Gambino, K. J. Healey and S. Nandi, *Precision Determination of the Cabibbo-Kobayashi-Maskawa Element* V_{cb}, *Phys. Rev. Lett.* **114** (2015) 061802, [1411.6560].

[13] P. Gambino, K. J. Healey and S. Turczyk, *Taming the higher power corrections in semileptonic B decays*, *Phys. Lett. B* **763** (2016) 60–65, [1606.06174].

[14] BaBar collaboration, B. Aubert et al., *Measurement of the Decay $B^- \to D^{*0} e^- \bar{\nu}_e$*, *Phys. Rev. Lett.* **100** (2008) 231803, [0712.3493].

[15] BaBar collaboration, B. Aubert et al., *Determination of the form-factors for the decay $B^0 \to D^{*-} \ell^+ \nu_l$ and of the CKM matrix element $|V_{cb}|$*, *Phys. Rev. D* **77** (2008) 032002, [0705.4008].

[16] BaBar collaboration, B. Aubert et al., *Measurements of the Semileptonic Decays $\bar{B} \to D \ell \bar{\nu}$ and $\bar{B} \to D^* \ell \bar{\nu}$ Using a Global Fit to $DX \ell \bar{\nu}$ Final States*, *Phys. Rev. D* **79** (2009) 012002, [0809.0828].

[17] BaBar collaboration, B. Aubert et al., *Measurement of $|V_{cb}|$ and the Form-Factor Slope in $\bar{B} \to D \ell^- \bar{\nu}_\ell$ Decays in Events Tagged by a Fully Reconstructed B Meson*, *Phys. Rev. Lett.* **104** (2010) 011802, [0904.4063].

[18] Belle collaboration, W. Dungel et al., *Measurement of the form factors of the decay $B^0 \to D^{*-} \ell^+ \nu_\ell$ and determination of the CKM matrix element $|V_{cb}|$*, *Phys. Rev. D* **82** (2010) 112007, [1010.5620].

[19] Belle collaboration, R. Glattauer et al., *Measurement of the decay $B \to D \ell \nu_\ell$ in fully reconstructed events and determination of the Cabibbo-Kobayashi-Maskawa matrix element $|V_{cb}|$*, *Phys. Rev. D* **93** (2016) 032006, [1510.03657].

[20] Belle collaboration, A. Abdesselam et al., *Precise determination of the CKM matrix element $|V_{cb}|$ with $\bar{B}^0 \to D^{*+} \ell^- \bar{\nu}_\ell$ decays with hadronic tagging at Belle*, 1702.01521.

[21] Belle collaboration, E. Waheed et al., *Measurement of the CKM matrix element $|V_{cb}|$ from $B^0 \to D^{*-} \ell^+ \nu_\ell$ at Belle*, *Phys. Rev. D* **100** (2019) 052007, [1809.03290].

[22] HFLAV collaboration, Y. S. Amhis et al., *Averages of b-hadron, c-hadron, and τ-lepton properties as of 2018*, *Eur. Phys. J. C* **81** (2021) 226, [1909.12524].

[23] BaBar collaboration, J. P. Lees et al., *Evidence for an excess of $\bar{B} \to D^{(*)} \tau^- \bar{\nu}_\tau$ decays*, *Phys. Rev. Lett.* **109** (2012) 101802, [1205.5442].

[24] BaBar collaboration, J. P. Lees et al., *Measurement of an Excess of $\bar{B} \to D^{(*)} \tau^- \bar{\nu}_\tau$ Decays and Implications for Charged Higgs Bosons*, *Phys. Rev. D* **88** (2013) 072012, [1303.0571].

[25] LHCb collaboration, R. Aaij et al., *Measurement of the ratio of branching fractions $\mathcal{B}(\bar{B}^0 \to D^{*+} \tau^- \bar{\nu}_\tau)/\mathcal{B}(\bar{B}^0 \to D^{*+} \mu^- \bar{\nu}_\mu)$*, *Phys. Rev. Lett.* **115** (2015) 111803, [1506.08614].

[26] Belle collaboration, M. Huschle et al., *Measurement of the branching ratio of $\bar{B} \to D^{(*)} \tau^- \bar{\nu}_\tau$ relative to $\bar{B} \to D^{(*)} \ell^- \bar{\nu}_\ell$ decays with hadronic tagging at Belle*, *Phys. Rev. D* **92** (2015) 072014, [1507.03233].

[27] Belle collaboration, Y. Sato et al., *Measurement of the branching ratio of $\bar{B}^0 \to D^{*+} \tau^- \bar{\nu}_\tau$ relative to $\bar{B}^0 \to D^{*+} \ell^- \bar{\nu}_\ell$ decays with a semileptonic tagging method*, *Phys. Rev. D* **94** (2016) 072007, [1607.07923].

[28] Belle collaboration, S. Hirose et al., *Measurement of the τ lepton polarization and $R(D^*)$ in the decay $\bar{B} \to D^* \tau^- \bar{\nu}_\tau$*, *Phys. Rev. Lett.* **118** (2017) 211801, [1612.00529].

[29] LHCb collaboration, R. Aaij et al., *Measurement of the ratio of the $B^0 \to D^{*-} \tau^+ \nu_\tau$ and $B^0 \to D^{*-} \mu^+ \nu_\mu$ branching fractions using three-prong τ-lepton decays*, *Phys. Rev. Lett.* **120** (2018) 171802, [1708.08856].

[30] Belle collaboration, S. Hirose et al., *Measurement of the τ lepton polarization and $R(D^*)$ in the decay $\bar{B} \to D^* \tau^- \bar{\nu}_\tau$ with one-prong hadronic τ decays at Belle*, *Phys. Rev. D* **97** (2018) 012004, [1709.00129].

[31] LHCb collaboration, R. Aaij et al., *Test of Lepton Flavor Universality by the measurement of the $B^0 \to D^{*-} \tau^+ \nu_\tau$ branching fraction using three-prong τ decays*, *Phys. Rev. D* **97** (2018) 072013, [1711.02505].

[32] LHCb collaboration, R. Aaij et al., *Test of lepton universality in beauty-quark decays*, *Nature Phys.* **18** (2022) 277–282, [2103.11769].

[33] LHCb collaboration, R. Aaij et al., *Tests of lepton universality using $B^0 \to K^0_S \ell^+ \ell^-$ and $B^+ \to K^{*+} \ell^+ \ell^-$ decays*, *Phys. Rev. Lett.* **128** (2022) 191802, [2110.09501].

[34] LHCb collaboration, R. Aaij et al., *Test of lepton universality with $B^0 \to K^{*0} \ell^+ \ell^-$ decays*, *JHEP* **08** (2017) 055, [1705.05802].

[35] Belle collaboration, A. Abdesselam et al., *Test of Lepton-Flavor Universality in $B \to K^* \ell^+ \ell^-$ Decays at Belle*, *Phys. Rev. Lett.* **126** (2021) 161801, [1904.02440].

[36] RBC, UKQCD collaboration, R. Abbott et al., *Direct CP violation and the $\Delta I = 1/2$ rule in $K \to \pi\pi$ decay from the standard model*, *Phys. Rev. D* **102** (2020) 054509, [2004.09440].

[37] M. Ciuchini, E. Franco, V. Lubicz, G. Martinelli, L. Silvestrini and C. Tarantino, *Power corrections to the CP-violation parameter ε_K*, *JHEP* **02** (2022) 181, [2111.05153].

[38] Particle Data Group collaboration, R. L. Workman et al., *Review of Particle Physics*, *PTEP* **2022** (2022) 083C01.

[39] Flavour Lattice Averaging Group (FLAG) collaboration, Y. Aoki et al., *FLAG Review 2021*, *Eur. Phys. J. C* **82** (2022) 869, [2111.09849].

[40] M. Bordone, B. Capdevila and P. Gambino, *Three loop calculations and inclusive V_{cb}*, *Phys. Lett. B* **822** (2021) 136679, [2107.00604].

[41] T. Blum et al., *$K \to \pi\pi$ $\Delta I = 3/2$ decay amplitude in the continuum limit*, *Phys. Rev. D* **91** (2015) 074502, [1502.00263].

[42] J. de Blas, M. Pierini, L. Reina and L. Silvestrini, *Impact of the recent measurements of the top-quark and W-boson masses on electroweak precision fits*, 2204.04204.

[43] M. Moulson, *Experimental determination of V_{us} from kaon decays*, *PoS* **CKM2016** (2017) 033, [1704.04104].

[44] W. J. Marciano and A. Sirlin, *Improved calculation of electroweak radiative corrections and the value of V_{ud}*, *Phys. Rev. Lett.* **96** (2006) 032002, [hep-ph/0510099].

[45] C.-Y. Seng, M. Gorchtein, H. H. Patel and M. J. Ramsey-Musolf, *Reduced Hadronic Uncertainty in the Determination of V_{ud}*, *Phys. Rev. Lett.* **121** (2018) 241804, [1807.10197].

[46] C. Y. Seng, M. Gorchtein and M. J. Ramsey-Musolf, *Dispersive evaluation of the inner radiative correction in neutron and nuclear β decay*, *Phys. Rev. D* **100** (2019) 013001, [1812.03352].

[47] A. Czarnecki, W. J. Marciano and A. Sirlin, *Radiative Corrections to Neutron and Nuclear Beta Decays Revisited*, *Phys. Rev. D* **100** (2019) 073008, [1907.06737].

[48] J. C. Hardy and I. S. Towner, *Superallowed $0^+ \to 0^+$ nuclear β decays: 2020 critical survey, with implications for V_{ud} and CKM unitarity*, *Phys. Rev. C* **102** (2020) 045501.

[49] D. Giusti, V. Lubicz, G. Martinelli, C. T. Sachrajda, F. Sanfilippo, S. Simula et al., *First lattice calculation of the QED corrections to leptonic decay rates*, *Phys. Rev. Lett.* **120** (2018) 072001, [1711.06537].

[50] M. Di Carlo, D. Giusti, V. Lubicz, G. Martinelli, C. T. Sachrajda, F. Sanfilippo et al., *Light-meson leptonic decay rates in lattice QCD+QED*, *Phys. Rev. D* **100** (2019) 034514, [1904.08731].

[51] G. D'Agostini, *Sceptical combination of experimental results: General considerations and application to ϵ'/ϵ*, hep-ex/9910036.

[52] R. J. Hudspith, R. Lewis, K. Maltman and J. Zanotti, *A resolution of the inclusive flavor-breaking τ $|V_{us}|$ puzzle*, *Phys. Lett. B* **781** (2018) 206–212, [1702.01767].

[53] K. Maltman et al., *Current Status of inclusive hadronic τ determinations of $|V_{us}|$*, *SciPost Phys. Proc.* **1** (2019) 006.

[54] V. Cirigliano, A. Crivellin, M. Hoferichter and M. Moulson, *Scrutinizing CKM unitarity with a new measurement of the $K_{\mu 3}/K_{\mu 2}$ branching fraction*, 2208.11707.

[55] M. Blanke and A. J. Buras, *Emerging ΔM_d -anomaly from tree-level determinations of $|V_{cb}|$ and the angle γ*, *Eur. Phys. J. C* **79** (2019) 159, [1812.06963].

[56] A. J. Buras and E. Venturini, *Searching for New Physics in Rare K and B Decays without $|V_{cb}|$ and $|V_{ub}|$ Uncertainties*, *Acta Phys. Polon. B* **53** (9, 2021) A1, [2109.11032].

[57] F. Bernlochner, M. Fael, K. Olschewsky, E. Persson, R. van Tonder, K. K. Vos et al., *First extraction of inclusive V_{cb} from q^2 moments*, *JHEP* **10** (2022) 068, [2205.10274].

[58] Fermilab Lattice, MILC collaboration, A. Bazavov et al., *Semileptonic form factors for $B \to D^* \ell\nu$ at nonzero recoil from 2 + 1-flavor lattice QCD*, 2105.14019.

[59] M. Di Carlo, G. Martinelli, M. Naviglio, F. Sanfilippo, S. Simula and L. Vittorio, *Unitarity bounds for semileptonic decays in lattice QCD*, *Phys. Rev. D* **104** (2021) 054502, [2105.02497].

[60] G. Martinelli, S. Simula and L. Vittorio, *Constraints for the semileptonic B→D(*) form factors from lattice QCD simulations of two-point correlation functions*, *Phys. Rev. D* **104** (2021) 094512, [2105.07851].

[61] G. Martinelli, S. Simula and L. Vittorio, *$|V_{cb}|$ and $R(D^{(*)})$ using lattice QCD and unitarity*, *Phys. Rev. D* **105** (2022) 034503, [2105.08674].

[62] G. Martinelli, M. Naviglio, S. Simula and L. Vittorio, *$|V_{cb}|$, lepton flavor universality and $SU(3)_F$ symmetry breaking in Bs→Ds(*)$\ell\nu_\ell$ decays through unitarity and lattice QCD*, *Phys. Rev. D* **106** (2022) 093002, [2204.05925].

[63] G. Martinelli, S. Simula and L. Vittorio, *Exclusive determinations of $|V_{cb}|$ and $R(D^*)$ through unitarity*, *Eur. Phys. J. C* **82** (2022) 1083, [2109.15248].

[64] P. Gambino, M. Jung and S. Schacht, *The V_{cb} puzzle: An update*, *Phys. Lett. B* **795** (2019) 386–390, [1905.08209].

[65] S. Jaiswal, S. Nandi and S. K. Patra, *Updates on extraction of $|V_{cb}|$ and SM prediction of R(D*) in $B \to D^* \ell\nu_\ell$ decays*, *JHEP* **06** (2020) 165, [2002.05726].

[66] A. Sirlin, *Large m_W, m_Z Behavior of the $O(\alpha)$ Corrections to Semileptonic Processes Mediated by W*, *Nucl. Phys. B* **196** (1982) 83–92.

[67] Belle-II collaboration, K. Adamczyk et al., *Determination of $|V_{ub}|$ from untagged $B^0 \to \pi^- \ell^+ \nu_\ell$ decays using 2019-2021 Belle II data*, 2210.04224.

[68] Fermilab Lattice, MILC collaboration, J. A. Bailey et al., *$|V_{ub}|$ from $B \to \pi\ell\nu$ decays and (2+1)-flavor lattice QCD*, *Phys. Rev. D* **92** (2015) 014024, [1503.07839].

[69] J. M. Flynn, T. Izubuchi, T. Kawanai, C. Lehner, A. Soni, R. S. Van de Water et al., *$B \to \pi\ell\nu$ and $B_s \to K\ell\nu$ form factors and $|V_{ub}|$ from 2+1-flavor lattice QCD with domain-wall light quarks and relativistic heavy quarks*, *Phys. Rev. D* **91** (2015) 074510, [1501.05373].

[70] JLQCD collaboration, B. Colquhoun, S. Hashimoto, T. Kaneko and J. Koponen, *Form factors of B→πℓν and a determination of $|V_{ub}|$ with Möbius domain-wall fermions*, *Phys. Rev. D* **106** (2022) 054502, [2203.04938].

[71] UTfit collaboration, M. Bona et al., *The Unitarity Triangle Fit in the Standard Model and Hadronic Parameters from Lattice QCD: A Reappraisal after the Measurements of Δm_s and $BR(B \to \tau\nu_\tau)$*, *JHEP* **10** (2006) 081, [hep-ph/0606167].

[72] T. Inami and C. S. Lim, *Effects of Superheavy Quarks and Leptons in Low-Energy Weak Processes $K_L \to \mu\bar{\mu}$, $K^+ \to \pi^+ \nu\bar{\nu}$ and $K^0 \leftrightarrow \bar{K}^0$*, *Prog. Theor. Phys.* **65** (1981) 297.

[73] J. Brod, M. Gorbahn and E. Stamou, *Standard-Model Prediction of ϵ_K with Manifest Quark-Mixing Unitarity*, *Phys. Rev. Lett.* **125** (2020) 171803, [1911.06822].

[74] A. J. Buras and D. Guadagnoli, *Correlations among new CP violating effects in $\Delta F = 2$ observables*, *Phys. Rev. D* **78** (2008) 033005, [0805.3887].

[75] RBC, UKQCD collaboration, N. H. Christ, *Long-distance contributions to weak amplitudes*, in *28th International Symposium on Lattice Field Theory*, 12, 2010. 1012.6034.

[76] N. H. Christ, X. Feng, G. Martinelli and C. T. Sachrajda, *Effects of finite volume on the K_L-K_S mass difference*, *Phys. Rev. D* **91** (2015) 114510, [1504.01170].

[77] N. H. Christ and Z. Bai, *Computing the long-distance contributions to ε_K*, *PoS* **LATTICE2015** (2016) 342.

[78] A. J. Buras, D. Guadagnoli and G. Isidori, *On ϵ_K Beyond Lowest Order in the Operator Product Expansion*, *Phys. Lett. B* **688** (2010) 309–313, [1002.3612].

[79] J. Brod, S. Kvedaraite, Z. Polonsky and A. Youssef, *Electroweak Corrections to the Charm-Top-Quark Contribution to ϵ_K*, 2207.07669.

[80] J. Brod and M. Gorbahn, *ϵ_K at Next-to-Next-to-Leading Order: The Charm-Top-Quark Contribution*, *Phys. Rev. D* **82** (2010) 094026, [1007.0684].

[81] J. Brod and M. Gorbahn, *Next-to-Next-to-Leading-Order Charm-Quark Contribution to the CP Violation Parameter ϵ_K and ΔM_K*, *Phys. Rev. Lett.* **108** (2012) 121801, [1108.2036].

[82] G. Martinelli, C. Pittori, C. T. Sachrajda, M. Testa and A. Vladikas, *A General method for nonperturbative renormalization of lattice operators*, *Nucl. Phys. B* **445** (1995) 81–108, [hep-lat/9411010].

[83] C. Sturm, Y. Aoki, N. H. Christ, T. Izubuchi, C. T. C. Sachrajda and A. Soni, *Renormalization of quark bilinear operators in a momentum-subtraction scheme with a nonexceptional subtraction point*, *Phys. Rev. D* **80** (2009) 014501, [0901.2599].

[84] M. Ciuchini, E. Franco, G. Martinelli and L. Reina, *The $\Delta S = 1$ effective Hamiltonian including next-to-leading order QCD and QED corrections*, *Nucl. Phys. B* **415** (1994) 403–462, [hep-ph/9304257].

[85] A. J. Buras, M. Jamin, M. E. Lautenbacher and P. H. Weisz, *Effective Hamiltonians for $\Delta S = 1$ and $\Delta B = 1$ nonleptonic decays beyond the leading logarithmic approximation*, *Nucl. Phys. B* **370** (1992) 69–104.

[86] A. J. Buras, M. Jamin, M. E. Lautenbacher and P. H. Weisz, *Two loop anomalous dimension matrix for $\Delta S = 1$ weak nonleptonic decays I: $\mathcal{O}(\alpha_s^2)$*, *Nucl. Phys. B* **400** (1993) 37–74, [hep-ph/9211304].

[87] G. Buchalla, A. J. Buras and M. E. Lautenbacher, *Weak decays beyond leading logarithms*, *Rev. Mod. Phys.* **68** (1996) 1125–1144, [hep-ph/9512380].

[88] V. Cirigliano, H. Gisbert, A. Pich and A. Rodríguez-Sánchez, *Isospin-violating contributions to ϵ'/ϵ*, *JHEP* **02** (2020) 032, [1911.01359].

[89] C. Lehner and C. Sturm, *Matching factors for $\Delta S = 1$ four-quark operators in RI/SMOM schemes*, *Phys. Rev. D* **84** (2011) 014001, [1104.4948].

[90] M. Ciuchini, M. Pierini and L. Silvestrini, *The Effect of penguins in the $B_d \to J/\psi K^0$ CP asymmetry*, *Phys. Rev. Lett.* **95** (2005) 221804, [hep-ph/0507290].

[91] A. J. Buras, P. Gambino, M. Gorbahn, S. Jager and L. Silvestrini, *Universal unitarity triangle and physics beyond the standard model*, *Phys. Lett. B* **500** (2001) 161–167, [hep-ph/0007085].

[92] G. Martinelli, S. Simula and L. Vittorio, *Exclusive semileptonic $B \to \pi \ell \nu_\ell$ and $B_s \to K \ell \nu_\ell$ decays through unitarity and lattice QCD*, *JHEP* **08** (2022) 022, [2202.10285].